MODELING PARAMETERS FOR THE NONLINEAR SEISMIC ANALYSIS OF REINFORCED CONCRETE COLUMNS RETROFITTED USING FRP OR STEEL JACKETING

by

José C. Alvarez and Sergio F. Breña

Department of Civil and Environmental Engineering
University of Massachusetts Amherst

Report submitted to the
Concrete Research Council of the
ACI Foundation
(CRC Project Report no. 71)

October 2017

Acknowledgment

Funding for this research project was provided by the Concrete Research Council of the ACI Foundation. This support is greatly appreciated. The first author would like to express gratitude for the additional support provided by the NEAGEP at the University of Massachusetts Amherst, which enabled him to complete his PhD Degree.

Abstract

The use of nonlinear analysis procedures in the analysis of reinforced concrete buildings subjected to seismic retrofitting is commonly used for design. To approximately capture the nonlinear response of structural elements, backbone (envelope) curves are used. Procedures to construct backbone curves for existing components of frames (beams, joints, and columns) have been extensively researched over the years. In contrast, recommendations to construct backbone curves for retrofitted components are largely lacking. The research in this project was intended to assist in filling this gap in knowledge.

This report presents recommendations to construct backbone curves of circular and rectangular retrofitted columns using jacketing materials within the context of *ASCE/SEI 41-13* and *ACI 369R-11*. The recommendations are based on a study of the characteristics of the hysteretic response of jacketed columns determined through past laboratory testing. Backbone curves were constructed using these data and determining key parameters that the multi-linear characteristics of these envelope curves. Drift and lateral strength at three key points that were used to approximately define the backbone curve of jacketed columns were selected. The three points selected for this study correspond to yielding, strength and residual strength after loss of lateral-load carrying capacity.

Force and drift at yield, strength, and residual strength were determined using two different methods. Force values at yield and peak strength were computed using accepted sectional models that use nominal material properties. The results from these models were compared with values extracted from tests of jacketed columns available in the literature. The residual strength was approximately defined as 20% of the peak strength. Drift values at the three key points were established from a statistical study of measured values of laboratory tests found in the literature. The drift data were fit to three different probability distributions and the one that best fit the laboratory data was used to construct fragility curves for plastic drift of jacketed columns. These curves were then used to propose the value of drift at the probability of exceedance of 0.5.

The research presented in this report can be used to develop backbone curves of jacketed columns using steel or FRP jackets consistent with *ACI 369.1-11* and *ASCE/SEI 41-13*. It is hoped that the study will facilitate future updates to these documents by including nonlinear modeling procedures for jacketed columns.

Table of Contents

LIST OF TABLES

LIST OF FIGURES

CHAPTER 1 INTRODUCTION

Experimental research on jacketed reinforced concrete (RC) columns has demonstrated that the behavior of retrofitted RC columns can be adequate to resist seismic loading. Increases in strength and ductility have been achieved when jackets are applied to deficient columns with details typical of pre-1971 code provisions. Typically, deficiencies found in older columns include low shear strength, insufficient core confinement, and short lap-splices within the plastic hinge region. Columns with these deficiencies usually exhibit brittle failures at limited displacement ductility (μ_Δ) with values typically lower than 2, a displacement ductility that is insufficient to dissipate considerable energy during the incidence of seismic loading. Jacketed columns have been observed to develop μ_Δ of 4 or greater.

The jacket materials selected to study in this research are constructed using steel or fiber reinforced polymer (FRP) materials. These two jacket types have been widely used and accepted to retrofit columns with deficient detailing. The mechanical properties of steel and the material deformation capacity are beneficial to column jacketing. The mechanical properties of FRP materials, including its high unidirectional strength and high elastic modulus, and its light weight makes FRP jackets attractive for use in columns. Both types of jackets are applied externally and minimally affect the size of retrofitted components.

To adequately capture the nonlinear hysteretic behavior of jacketed RC columns, an understanding of the interaction between the jacket materials and the existing column is required. To this date there are no common recommendations to model the hysteretic behavior of jacketed columns. Furthermore, jacket parameters needed to develop a specified displacement ductility are difficult to define. Defining the influenced of these parameters is important to develop backbone curves that envelope the hysteretic curves that describe the nonlinear behavior of jacketed columns.

Jacketed RC columns have a composite behavior which can be complicated to model in a finite element analysis (FEA) program accurately. Past studies have developed different numerical and physical models that attempt to capture the confining effects and shear strength of jacketed columns. The models use procedures developed specifically from the experimental testing that was conducted in each study. The goal of this study is to provide recommendations to model jacketed RC columns with different detailing and jacketing materials so that backbone curves can be constructed. To construct force-deformation backbone curves, the strength and ductility at key points of the backbone needs definition. This study will attempt to develop procedures that will assist in the definition of the coordinates (force-displacement) of backbone curves for jacketed columns. The force-deformation curves can then be used in combination with hysteretic rules to model the nonlinear behavior of jacketed columns.

1.1 Motivation

Poorly detailed columns are prone to axial load failures or shear failures in active seismic areas around the world. Structures designed using older (pre-1970) code provisions may be susceptible to severe seismic damage (Figure 1-1). The research in this report concentrates on retrofitting deficient RC columns by jacketing columns to improve their seismic performance and prevent the possible collapse of a structure. Only jackets fabricated using FRP or steel material are considered because of their prevalence in practice.

Figure 2-1 Reinforced concrete column crushing

Jacketing is a widely accepted method for retrofitting RC columns. The increase in shear strength and confinement, and improved lap-splice performance without creating a significant impact on the column dimensions makes them attractive compared with other retrofitting techniques. To verify the performance of structures containing jacketed columns, non-linear modeling parameters for jacketed columns that incorporate the effects of jacketing materials and column cross-section geometry are needed. To develop these nonlinear modeling parameters, this research study focused on developing a database containing test results from jacketed columns to extract key points in the hysteretic behavior of these components measured during the tests. Models of jacketed columns that have been proposed by previous researchers are also included in the literature review.

1.2 Research Objective

The main objective of this research was to develop recommendations that can be used to construct backbone curves of jacketed columns using FRP or steel jackets. These backbone curves could then be used to model the nonlinear behavior of frames containing jacketed columns to assess the behavior of retrofitted structures. The study concentrated on developing backbone curves consistent with *ASCE/SEI 41-06* and *ACI 369.1-11* so that the procedure can be easily adopted into future editions of these documents.

CHAPTER 2 DATABASE OF JACKETED COLUMNS AND BACKBONE PARAMETERS

This chapter presents the procedure that was followed to construct a database of force-deformation backbone curves of jacketed reinforced concrete (RC) columns based on a large number of column specimens that were collected from the literature. The chapter begins with a brief description of the jacketing configurations and column characteristics used in the literature followed by a description of the column parameters in the database, and a description of the column backbone and key parameters included in the database.

2.1 Jacket Retrofit Configurations

Column retrofits using jacketing are intended to correct deficiencies in column original designs that may negatively impact their deformation capacity. The most common deficiencies encountered in columns designed with pre-1970s provisions are: short lap splices of longitudinal bars in plastic hinge regions, low shear strength, and insufficient confinement of the column core. Past researchers (Seible et al. 1997, Aboutaha 1999, Xiao 1997, Priestly et al. 1996, Chai et al. 1991, Harries et al. 2006, Elsnadedy and Haroun 2006) have based the recommendations for the jacket design to try to emulate the behavior of well-detailed columns. Figure 2-1 shows different basic arrangements used by past researchers to mitigate the different deficiencies by using either FRP jackets or steel jackets. Figure 2-1a shows a column with a full-height (continuous) jacket and Figure 2-1b shows a column with a jacket applied only in the potential plastic hinge regions of the column (partial-height jacket). A full-height jacket configuration would typically be used when concerns exist about the shear strength of the column and the partial-height jacket configuration is used if confinement and lap-splice improvement is needed in the plastic hinge zones of a column subjected to double curvature bending. These two configurations have been used and studied in past experimental studies depending on the deficiency encountered in the columns. It is important to note that a column that might not be initially considered deficient in shear could become deficient if the flexural strength is increased significantly as a result of jacketing the plastic hinge regions. Therefore the flexural strength of the jacketed column needs to be determined to assess whether the retrofitted column requires shear strengthening as well.

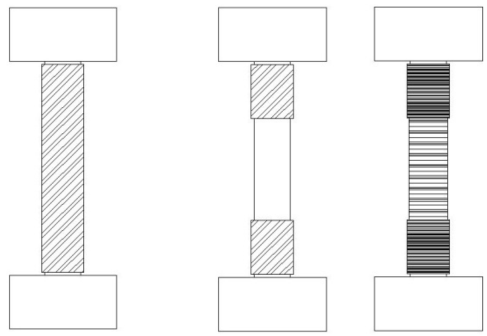

(a) (b) (c)

Figure 2-1 Typical jacket configurations

The jacket arrangements shown in Figure 2-1 apply to both steel and FRP material jackets. Unlike steel jackets, the thickness of FRP jackets can easily be varied along the height of the column (Figure 2-1c) because these materials can be laid up in the field. Having a steel jacket with variable thickness along the height is more difficult to accomplish.

2.2 Description of Jacketed Column Database

A jacketed column database was created in this research so that nonlinear parameters could be extracted from the test results. The database was compiled from publications and research reports that included tests of jacketed columns subjected to quasi-static lateral loading. The basic information that was collected from available publications were column geometry, material properties, reinforcement details and jacket details.

The publications typically reported the cyclic force-deformation response of jacketed column specimens in the form of graphs or tables. This information was used to construct a response envelope (backbone curve). The backbone was then used to extract yield force and peak force for comparison with existing strength models (Chapter 3). The backbone was also used to determine the deformation capacity of jacketed columns to conduct a statistical analysis that could be then used to propose drift values corresponding to different force levels (Chapter 4).

All the columns contained in the database were tested under lateral cyclic static loading applied incrementally following a prescribed loading protocol. Some columns were tested in as-built (un-retrofitted) conditions for comparison with the behavior of companion specimens employing jackets. The jackets studied were constructed using fiber-reinforced polymer (FRP) or steel materials. Columns were loaded in either single curvature bending (cantilever) or double curvature bending (fixed-fixed). These boundary conditions were meant to replicate the conditions of bridge columns or frame columns. Although this research is primarily directed to frame column retrofits the tests intended to simulate bridge column behavior (single curvature) were still included in the database because these columns may be considered representative of a column in a frame up to the point of inflection.

The database consists of a total of 116 columns, 84 and 32 columns jacketed using fiber reinforced polymer (FRP) or steel materials, respectively. Details of all the columns in the database are included in Appendix B. Figure 2-2a shows histograms that summarize the number of columns in the database according to jacket type and cross sectional geometry, and Figure 2-2b shows the number of columns classified by the deficiency encountered in the original design. The column deficiency is defined as a characteristic in the column design that is the cause of the failure of the column at a low displacement ductility.

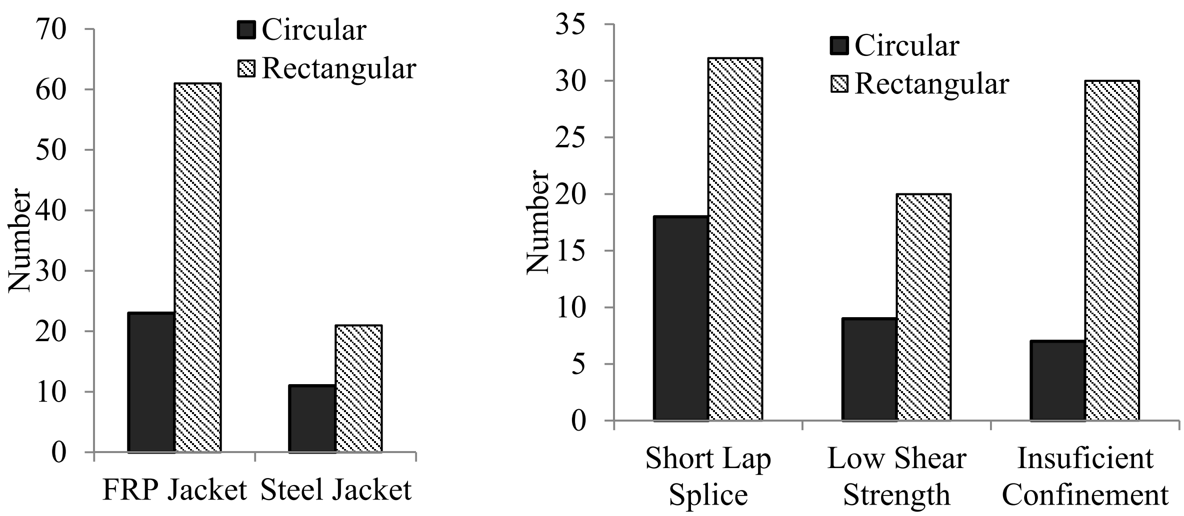

(a) (b)

Figure 2-2 Classification of columns in database

Table 2-1 and

Table 2-2 show the maximum and minimum values for different column parameters in the database. The parameters presented in these tables were selected because of they are known to influence column behavior. Parameters included in these tables are (1) spacing of transverse reinforcement (s) normalized by distance to the tension force resultant; (2) axial load ratio, defined as the axial load divided by the product of nominal compressive strength of the concrete (f'_c) times the gross cross-sectional area of the column (A_g); (3) jacket material used to retrofit the column (steel or FRP); and (4) ratio between shear at flexural

plastic hinging (V_o) and nominal shear strength (V_n). The nominal shear strength was calculated using the procedure proposed by Priestly et al. 1994 at a displacement ductility of 8 as described in Chapter 3. The shear demand corresponding to the formation of flexural plastic hinging was calculated using a moment-curvature analysis that incorporates the Mander et al. (1989) confinement model for concrete in compression. The nominal shear strength (V_n) did not include the contribution of the jacket in Table 2-1and

Table 2-2 because the ratios in these tables reflect the capacity of the as-built column to resist shear forces developed through the length of the column.

Table 2-1 Database maximum and minimun parameters for circular columns

	Steel Jackets Circular		FRP Jackets Circular	
No. of columns	11		23	
	Max	Min	Max	Min
Diameter (in)	29.90	24.00	24.00	9.50
Height (in)	144.00	72.00	144.00	37.50
f'_c (psi)	5800	3698	6500	2590
$P/A_g f'_c$	0.19	0.05	0.18	0.05
$\rho(\%)$	2.53	0.01	2.69	1.92
s/d	0.26	0.21	1.01	0.21
$\rho_v(\%)$	0.17	0.07	2.50	0.08
V_o/V_n	1.66	0.48	1.38	0.27

Table 2-2 Database maximum and minimun parameters for rectangular columns

	Steel Jackets Rectangular		FRP Jackets Rectangular	
No. of columns	21		61	
	Max	Min	Max	Min
b_c (in)	36.00	10.00	24.00	5.91
h_c (in)	36.00	10.00	28.74	7.87
h_c/b_c	2.00	0.50	2.00	1.00
Height (in)	144.00	40.00	144.02	39.37
f'_c (psi)	8702	2565	6802	1305
$P/A_g f'_c$	0.32	0.00	0.56	0.05
$\rho(\%)$	2.57	1.95	6.16	1.70
s/d	1.25	0.25	1.07	0.18
$\rho_v(\%)$	0.57	0.08	0.89	0.08
V_o/V_n	1.73	0.36	3.58	0.71

Closely spaced transverse reinforcement increases curvature ductility of columns by controlling buckling of longitudinal reinforcement after inelastic load reversals and by providing confinement of the concrete core. Axial load ratio ($P/A_gf'_c$) affects column behavior and may accentuate some of the deficiencies encountered in older columns. Columns subjected to high axial load ratios ($P/A_gf'_c > 0.15$) in combination with high lateral loads, may be affected by $P\text{-}\Delta$ effects that would limit the displacement capacity of these columns. On the other hand, columns with low levels of axial load ($P/A_gf'_c \leq 0.15$) could have a higher tension stress in the longitudinal bars, causing yielding at lower lateral displacement that could generate early onset of longitudinal bar slip for the same lateral load.

For the purposes of this research, a short lap splice is defined as a splice of the longitudinal reinforcement in the column within the plastic region of only 20 to 24 longitudinal bar diameters (d_b). These lengths have been found to be insufficient to avoid bar slippage when a column is subjected to inelastic load reversals. In older columns, splices were usually located within the plastic hinge zone of columns (above the foundation or above the floors) for ease of construction. Splices need to be sized to transfer tension forces in the presence of cyclic loading and contain closely spaced transverse reinforcement through the splice length to prevent splitting of concrete.

Widely spaced transverse reinforcement may cause columns to have low shear strength at large displacements. Shear critical columns are those that fail in shear at low displacement ductility before the development of the plastic hinges ($V_o > V_n$, $\mu_\Delta < 2$). Ductile shear design of columns in seismic regions should therefore be done with consideration of the flexural strength of the column to ensure that plastic hinging can occur and that the capacity of the column can be maintained.

2.3 Construction of Backbone Curves from Measured Hysteresis Curves

Column behavior from tests in the literature was reported as hysteresis force-deformation curves. From these hysteresis curves backbone (envelope) curves were constructed by digitizing data from the figures obtained from the original test references. The backbone curves were constructed using the force and displacement values measured during the first cycle at each displacement level. In some cases the authors of a paper directly reported backbone curves; these plots were digitized to obtain the force-deformation relationships instead of extracting them from hysteresis curves. Generation of a backbone curve from the response of one column in the database is illustrated in Figure 2-3. The backbone curves obtained for all the columns in the database are presented in Appendix A.

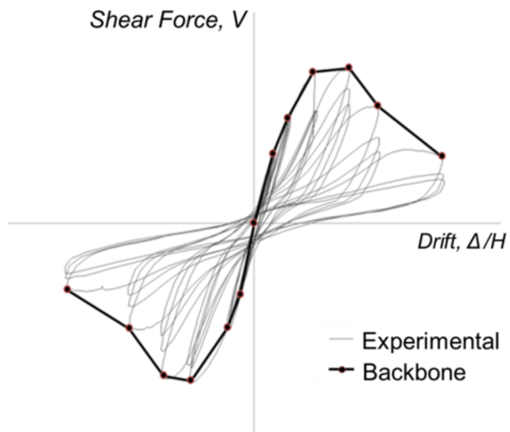

Figure 2-3 Backbone curve generated from experimental data

From each backbone curve, key points were extracted (Figure 2-4). The selected points are the yield strength and corresponding deformation, peak strength, plastic deformation to 20% loss in lateral strength (Parameter *a*), deformation from yield to loss of axial carrying capacity (Parameter *b*), residual strength (*c*) and maximum deformation. Parameter *a* was defined as the difference between the deformation at lateral strength degradation of 20% and the deformation at yield. In tests stopped before reaching a 20% drop in force from peak, Parameter *a* was defined as the maximum deformation imposed during the test. Parameter *b*, which corresponds to loss of axial capacity accompanied by a drop in lateral strength, could not be obtained from the literature because tests were typically stopped prior to reaching this level of strength degradation. Therefore, Parameter *b* was determined as the deformation corresponding to a degradation of 25% from the peak lateral load, V_{peak}. In cases where columns did not exhibit a strength degradation of more than 20%, Parameter *b* could not be determined and was set equal to the value in *ACI 369R-11* for existing columns.

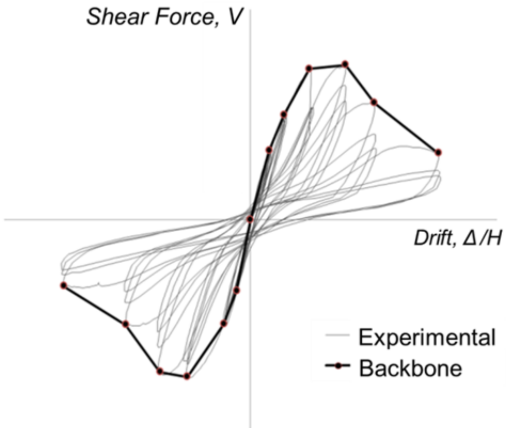

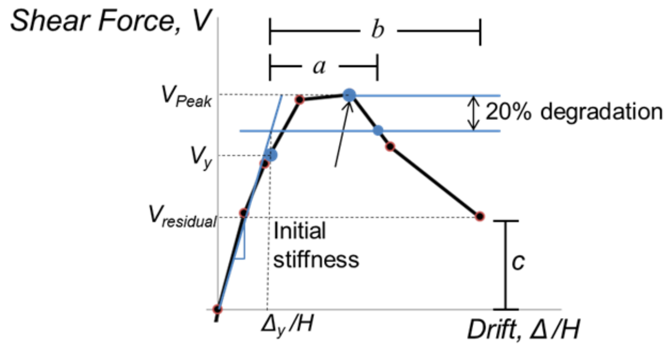

(a) (b)

Figure 2-4 Simplified backbone curve obtained from measured hysteretic response: (a) hysteresis curve with superimposed backbone (b) simplified nonlinear backbone curve and nonlinear parameters

The yield force and yield deformation of a column is defined analytically as the point at which the tension reinforcement located farthest from the neutral axis reaches its yield strain (first column yield). This value is reported by some researchers who instrumented the reinforcement in the test columns with strain gauges. This is not so in many of the columns in the database and therefore will not provide values of yield in a consistent manner. To have a general definition of yield for all columns in the database, the force and deformation at yield (V_y, Δ_y) were defined as the point in the measured force-deformation curve directly below the intersection of two secant lines. The first line was drawn through the origin using the same slope as the initial part of the force-deformation curve. The second line was dependent on the drift at peak. For columns that exhibited peak strength at a drift less than 2% with a limited increase in lateral force after yielding, V_y was defined as $0.8V_{peak}$. Alternately, for columns with a high increase in lateral force after yield (peak strength at drifts exceeding *3%*), V_y was defined as $0.7\ V_{peak}$. This procedure ensured that the V_y was near the end of the linear region in the force-deformation curve. The coordinates at peak force (V_{Peak}, Δ_{Peak}) were determined by using the average of the peaks measured in the positive and negative directions of loading. The residual force (V_{res} also known as parameter *c* in *ASCE/SEI 41-06*) and maximum displacement ($\Delta_{\max}$) were not typically reported in the literature of tests of jacketed columns. The experiments were often stopped when the column strength dropped under 80% of the peak force developed during the test. Therefore V_{res} was defined as the fraction representing 20% of the peak force (V_{peak}), and

Δ_{max} was defined conservatively as the maximum displacement reported for each tested column. It is expected that the majority of the columns would still be able to support larger displacements. Furthermore some tests were stopped because of limits on the testing equipment and not the column strength. **Error! Reference source not found.** In *ACI 369R-11* parameters *a, b* and *c* were determined from mean backbone values derived from a large number of reinforced column experiments (Elwood et al. 2007). Therefore mean values were also used to define the backbone parameters of jacketed columns. Figure 2-5 shows the mean parameters obtained from all retrofitted columns in the database according to jacketing material and cross-sectional shape. The parameters *a*, *b* and *c* from individual columns in the database are presented in the Appendix A. Because jacketed columns exhibited a gradual degradation to the point of loss of axial carrying capacity, the shape of the simplified backbone illustrated by a dashed line in Figure 2-6 was suggestedFigure 2-6.

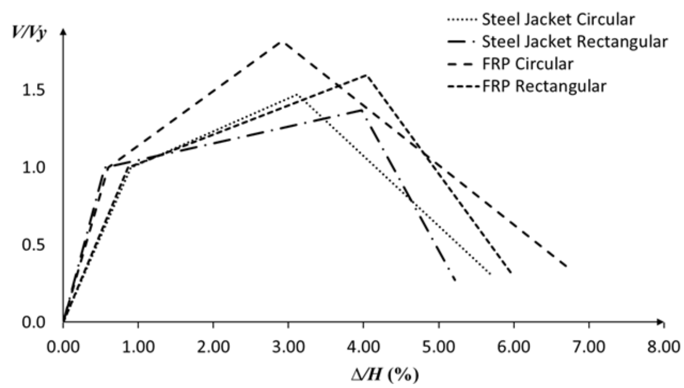

Figure 2-5 Mean force-deformation relationship of jacketed columns from database

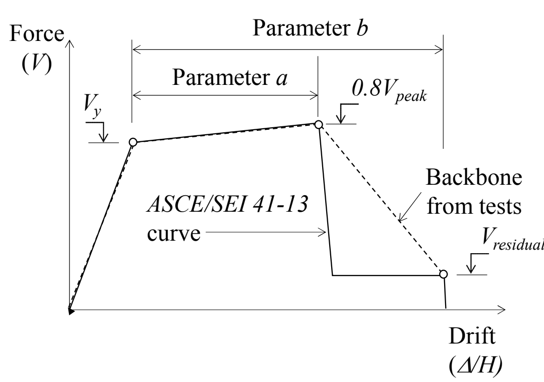

Figure 2-6 Proposed simplified force-deformation relationship of jacketed columns

CHAPTER 3 MODELS TO DETERMINE YIELD AND PEAK FORCE OF JACKETED COLUMNS

This chapter focuses on recommendations to determine the yield and peak force for jacketed columns. In this chapter the forces in jacketed columns obtained from the proposed models are compared with values extracted from the jacketed column database.

3.1 Calculation of Yield and Nominal Moments of Jacketed Columns

Cross-sectional models are typically used to estimate yield and nominal moment of reinforced concrete components. Cross-sectional strength can be calculated using fiber models wherein the cross section is divided into fibers and, for a given curvature of the cross section, the force in each fiber is calculated using the corresponding uniaxial material stress-strain laws. The model works by establishing equilibrium of internal forces to obtain the neutral axis location. Once the neutral axis depth in the cross section is established the forces in these fibers are used to calculate the internal moment developed by the cross section. The main purpose of the techniques described in this section was to develop a methodology that could be implemented into existing software that is used to compute the sectional strength of reinforced concrete (RC) columns containing internal reinforcement only.

Yield and nominal moments of a jacketed column cross section are affected by the jacket. Column jackets develop confining stresses in the concrete that have the effect of increasing the ultimate stress and ultimate strain of concrete. These confining stresses also provide a clamping effect on reinforcing bars that are spliced. To estimate yield moment and flexural strength of the cross section, a model that computes the confining pressure provided by the jacket and equates it to an equivalent quantity of internal transverse reinforcement was used (Figure 3-1and Figure 3-2). Models that capture concrete confining effects provided by internal transverse reinforcement (hoops) are widely available and currently implemented in available software such as Mander et al. (1988), Hoshikuma et al. (1997) and Madas and Elnasha (1991). In this research, the model developed by Mander et al. (1988) was used to estimate transverse reinforcing confining effects.

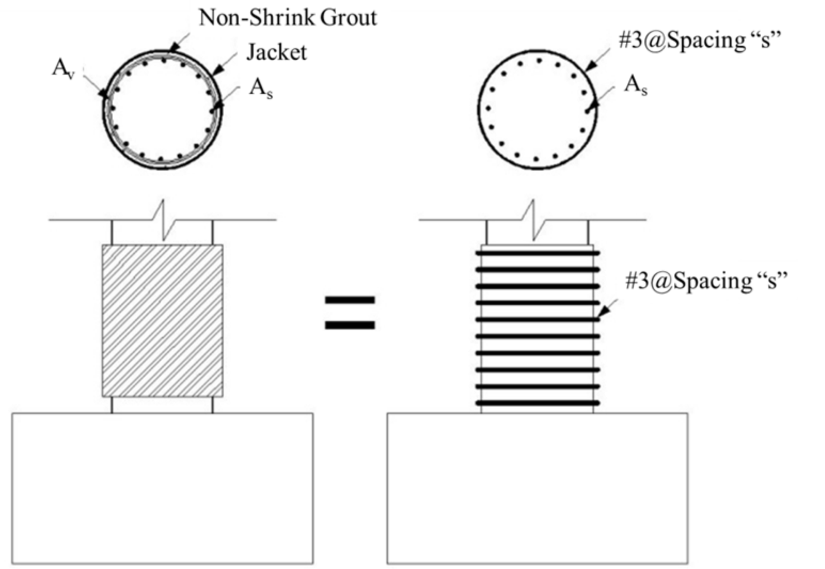

Figure 3-1 Circular jacketed column equivalent hoop spacing 's'

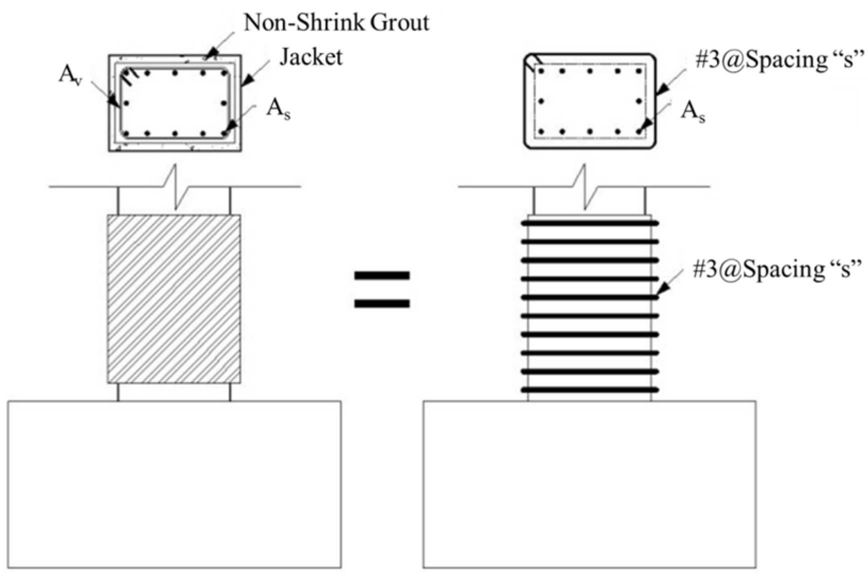

Figure 3-2 Rectangular jacketed column equivalent hoop spacing 's'

The Mander et al. (1988) model uses transverse reinforcement as well as commercial software to calculate the confining pressure. The confining pressure generated by internal transverse reinforcement following Mander et al. (1988) model for circular columns can be calculate with Eq. 3-1 and illustrated in Figure 3-3:

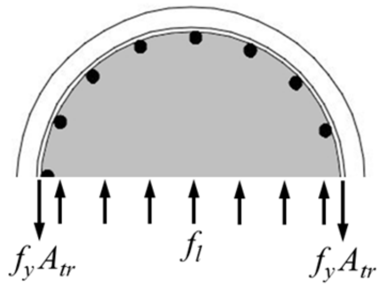

Figure 3-3 Confinement of concrete by circular hoops

$$f_l' = \frac{1}{2}\, k_e\, \rho_v\, f_y \qquad \textbf{Eq. 3-1}$$

In which ρ_v is:

$$\rho_v = \frac{4(A_{tr})}{D'\, s} \qquad \textbf{Eq. 3-2}$$

D' is the diameter of the internal hoops shown in Figure 3-4; k_e is an confinement efficiency factor that accounts for areas of concrete that are not confined along the length of the column as shown in Figure 3-4 and can be calculated using the following equation for circular columns with circular hoops:

$$k_e = \frac{\left(1 - \frac{s'}{2\,D'}\right)^2}{1 - \rho_s} \qquad \textbf{Eq. 3-3}$$

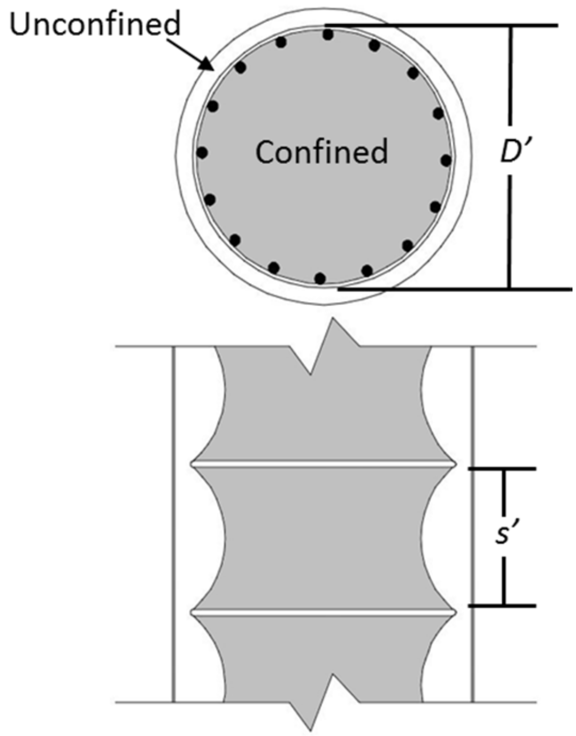

Figure 3-4 Circular column effective confined area

ρ_s is the longitudinal steel ratio calculated using the following equation:

$$\rho_s = \frac{A_s}{A_c} \qquad \textbf{Eq. 3-4}$$

A_c is the gross area of the concrete section, which for jacketed columns, calculated using the following equation for circular cross sections.

$$A_c = \frac{D^2 \pi}{4} \qquad \textbf{Eq. 3-5}$$

s is the distance between centerline of transverse reinforcement, but the Mander et al. (1988) model uses the clear spacing between transverse reinforcement (s') and therefore must add a bar diameter:

$$s = s' + d_b \qquad \textbf{Eq. 3-6}$$

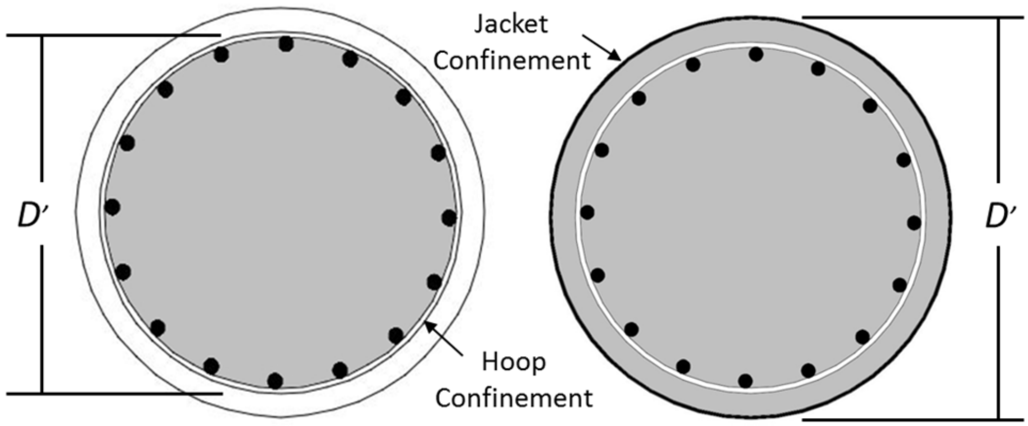

Figure 3-5 Confinement dimensions of jacketed column vs internal reinforcement

To use Eq. 3-1 to calculate the jacket contribution as show in

Figure 3-1 some modifications must be done to Mander et al. (1988). Tensile stresses are developed in the jacket instead of in transverse reinforcement illustrated in Figure 3-3; therefore the yield stress f_y of the jacket must be used in all equations. Jackets are applied externally so *D'* will be equal to the diameter of the jacketed column. Rectangular columns that have different side dimensions and different longitudinal and transverse reinforcement arrangement depending on the loading direction will have different confining stresses in the concrete in each direction (Figure 3-6). Figure 3-6 shows the physical representation of the confining stresses in the y direction. The effective confining stress provided by internal transverse reinforcement in the *x* and *y* directions of a rectangular column is given by (Mander et al. 1988) Eq. 3-7 and Eq. 3-8:

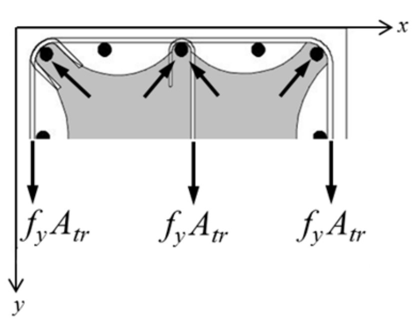

Figure 3-6 Confined area of a rectangular cross section

$$f_{lx} = k_e \rho_x f_{yh}$$ **Eq. 3-7**

$$f_{ly} = k_e \rho_y f_{yh}$$ **Eq. 3-8**

where ρ_x and ρ_y represent the transverse reinforcement content in the x ($A_{tr\text{-}x}/s{\cdot}d_c$) and y ($A_{tr\text{-}y}/s{\cdot}b_c$) directions, respectively; f_{yh} is the yield stress of transverse hoops; and k_e is an effectiveness factor to account for unconfined concrete zones in the vertical direction between hoops and in the horizontal direction between longitudinal reinforcing bar positions (Figure 3-7). This effectiveness factor may be estimated using:

$$k_e = b_c\, d_c \left(1 - \frac{\sum w_i^2}{6\, b_c\, d_c}\right)\left(1 - \frac{s'}{2\, b_c}\right)\left(1 - \frac{s'}{2\, d_c}\right) \qquad \textbf{Eq. 3-9}$$

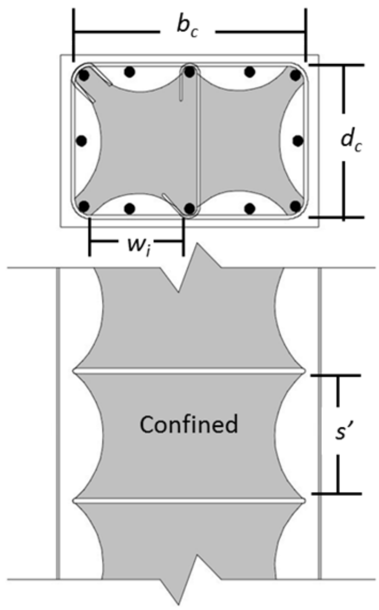

Figure 3-7 Rectangular columns effectively confined area

where b_c and d_c are the width and depth of the confined area as shown in Figure 3-7. The term Σw_i^2 is used to evaluate the reduction in confinement efficiency between longitudinal bars of the confined core as well as the reduction between transverse reinforcement.

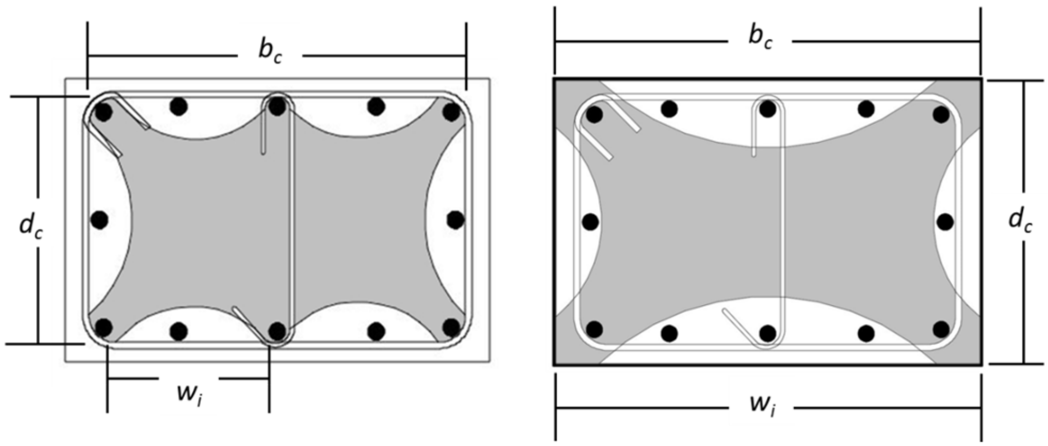

Figure 3-8 Confinement dimensions of jacketed columns vs internal reinforcement

Rectangular jackets, without anchors, only restrain the column corners, as shown in Figure 3-8, therefore the length of each side of the column cross-section is used to estimate $\sum w_i^2$, resulting in a value equal to $2\ b_c^2 + 2\ d_c^2$. Substituting this value into equation Eq. 3-9 gives:

$$k_e = b_c\ d_c \left(1 - \frac{2\ b_c^2 + 2\ d_c^2}{6\ b_c\ d_c}\right)\left(1 - \frac{s'}{2\ b_c}\right)\left(1 - \frac{s'}{2\ d_c}\right) \qquad \textbf{Eq. 3-10}$$

To obtain an equivalent transverse reinforcement for jacketed circular or rectangular columns, the confining pressure provided by the jacket (f_l) needs to be obtained. Once the jacket confining pressure acting on the concrete is estimated, the equations were solved for an equivalent hoop spacing (s) using the Mander et al. (1988) confinement model. The area of the equivalent transverse reinforcement and its spacing was obtained assuming no. 3 bars as equivalent transverse reinforcement.

Columns which contain spliced longitudinal reinforcement in the plastic hinge region were treated slightly differently; particularly those with short splice lengths. Older columns that typically contain short lap splice lengths (l_b) are not able to develop the strength of the longitudinal bars if the section is confined only using external jacketing. In order get accurate results, the stress that longitudinal reinforcement could develop was artificially reduced to be consistent with the maximum force that could be developed in the reinforcement at the onset of splice failure. A reduction to the yield stress of the longitudinal reinforcement as a function of lap length as proposed by Cho and Pincheira (2006) was used to take into account a splice length shorter than the development length (l_d) corresponding to reinforcing bar yielding. In Eq. 3-11 the design development length is decreased using a factor of 0.8, because development length equations in ACI 318-11 section 12.2 already contain a safety factor of 1.25. The relation between reinforcing bar stress developed as a function of lap splice length is not linear as indicated by the *2/3* power affecting the normalized lap length term in (Eq. 3-11).

$$f_s = \left(\frac{l_b}{0.8l_d}\right)^{2/3} f_y \qquad \textbf{Eq. 3-11}$$

By replacing the confining effect properties of a jacketed column with equivalent confining of internal transverse reinforcement, the moment-curvature analysis of the cross section can be calculated easily using commercial software. Because the jackets are applied externally the entire section of the column is assumed as confined as shown in Figure 3-9. This was achieved by specifying a concrete cover outside of the reinforcement equal to zero in the software.

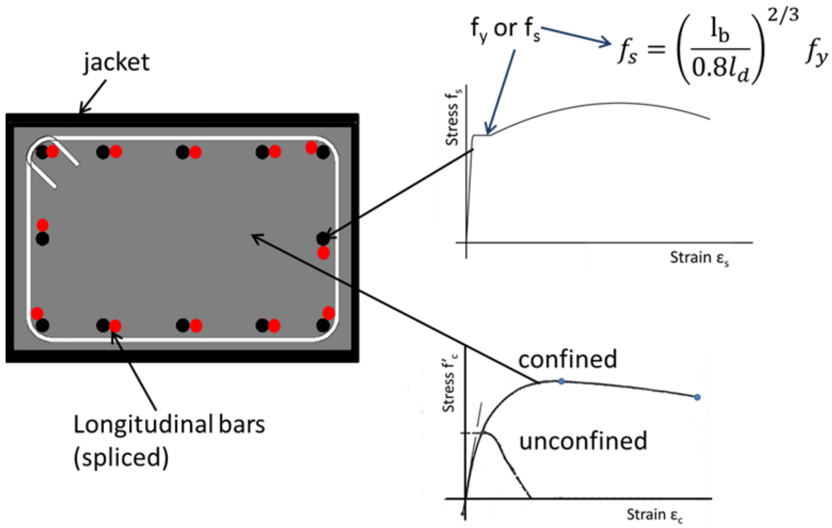

Figure 3-9 Figure 3-9 shows that the jacket was assumed not to contribute in the sectional flexural strength. Steel jackets have gaps at the bottom and top of the column (to avoid prying) limiting the development of significant stresses in the longitudinal direction and therefore are excluded from the sectional analysis. FRP material jackets are constructed with fibers oriented perpendicular to the column axis, prevents the jacket from contributing significantly to the column flexural strength.

Figure 3-10 illustrates the moment-curvature response of a jacketed column with FRP material. From the curve, the peak moment capacity and the yield moment of jacketed columns was obtained as illustrated.

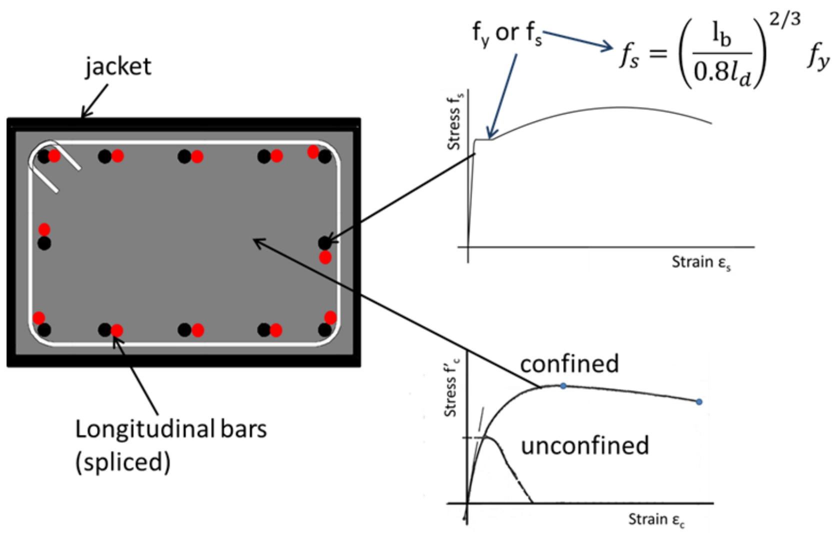

Figure 3-9 Assumed uniaxial stress-strain models

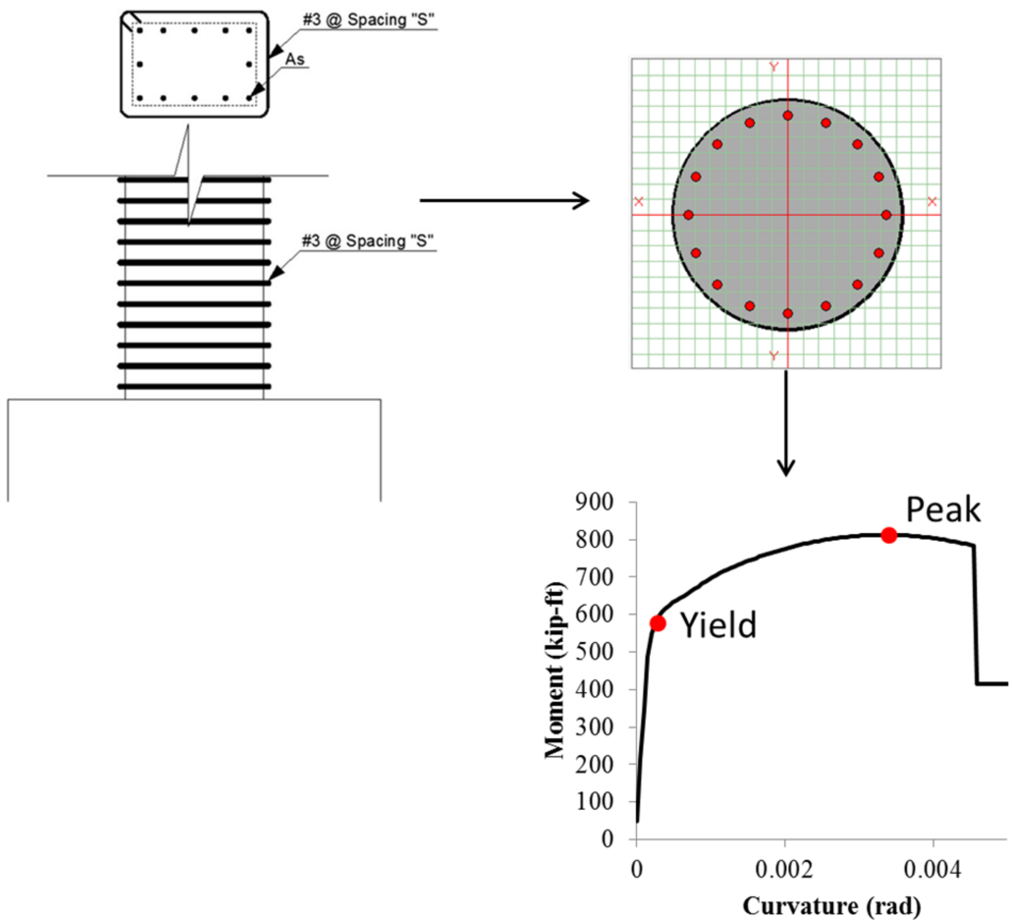

Figure 3-10 Jacketed column moment curvature analysis

The yield and peak force values determined the moment-curvature procedure described above were compared with measured values of the columns in the database. A comparison of calculated and measured values of yield and peak force are illustrated in Figure 3-11. The different symbols used in the figure depend on original column deficiency. Also, the four plots shown are for yield and peak forces of circular and rectangular columns. The plots illustrate that the majority of the data points lie close to a 45 degree line that represents a perfect fit. Most of the points lie within +/- 10% lines drawn in the figures.

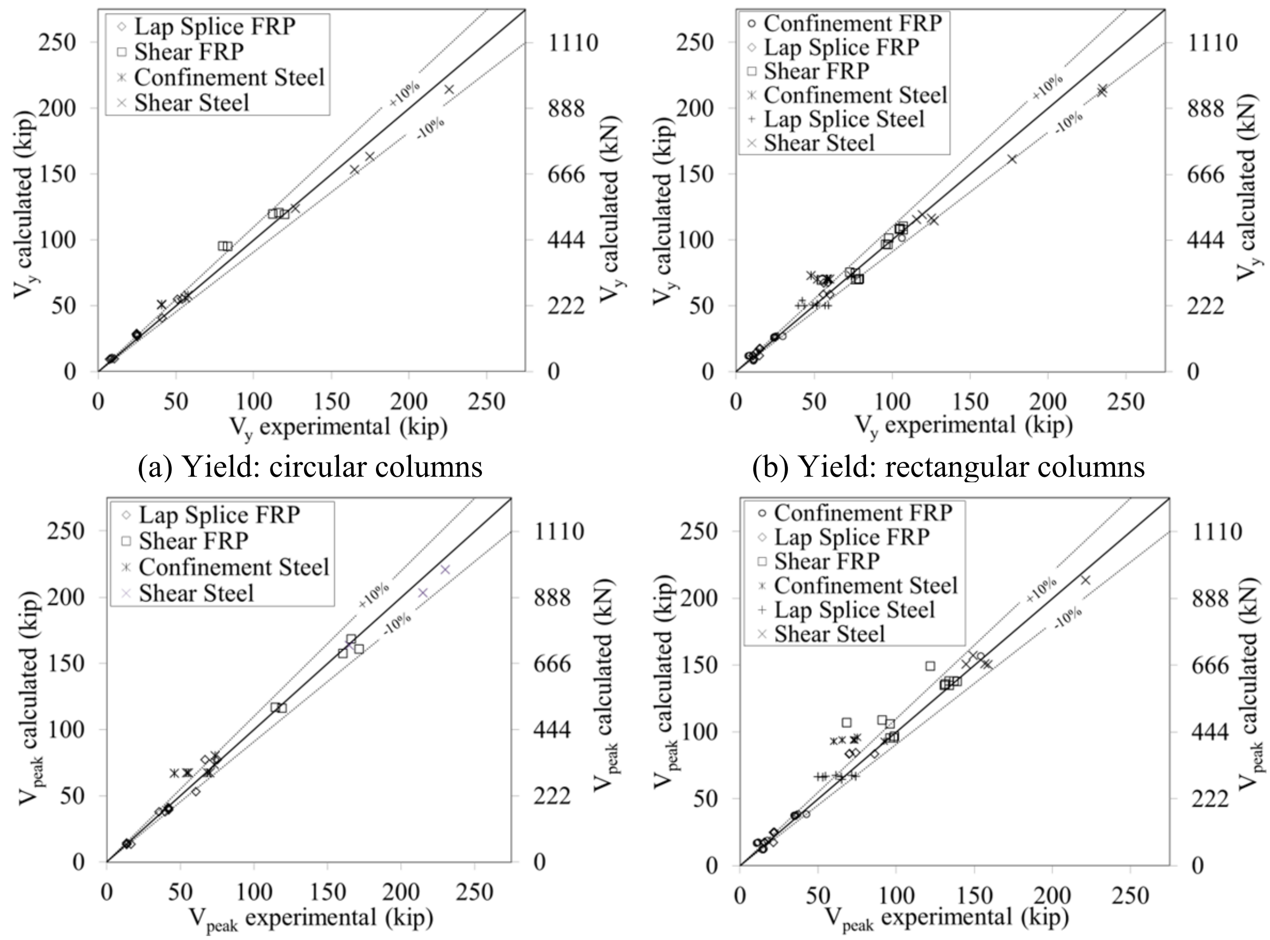

(a) Yield: circular columns

(b) Yield: rectangular columns

(c) Peak: circular columns

(d) Peak: rectangular columns

Figure 3-11 Comparison between calculated and experimental jacketed column strength: (a) and (b) shear at yield; (c) and (d) shear at peak strength

Table 3-1 and Table 3-2 summarize the comparisons of yield and peak force by jacket type and original column deficiency for circular and rectangular columns, respectively. Table 3-3 gives an overall summary of calculated and measured forces for all columns classified by jacket type. It can be seen that the proposed models better fit the values measured for steel-jacketed columns. Furthermore, for a specific jacket material, the calculated forces in circular columns are closer to values determined experimentally than those of rectangular columns.

Table 3-1 Comparison of circular column data by jacketing type

Circular Columns	Columns with Steel Jackets						Columns with FRP Jackets					
	Lap Splice		Shear		Confinement		Lap Splice		Shear		Confinement	
	Mean	STD	Mean	STD	Mean	STD	Mean	STD	Mean	STD	Mean	STD
Vy calc/Vy test	-	-	0.95	0.02	1.17	0.11	1.43	0.33	1.24	0.06	-	-
Vpeak calc/Vpeak test	-	-	0.98	0.04	1.13	0.17	1.23	0.24	0.99	0.03	-	-

Table 3-2 – Comparison of rectangular column data by jacketing type

Rectangular Columns	Columns with Steel Jackets						Columns with FRP Jackets					
	Lap Splice		Shear		Confinement		Lap Splice		Shear		Confinement	
	Mean	STD	Mean	STD	Mean	STD	Mean	STD	Mean	STD	Mean	STD
Vy calc/Vy test	1.33	0.25	0.95	0.04	1.47	0.43	2.17	0.73	1.39	0.19	1.24	0.24
Vpeak/Vpeak test	1.09	0.15	0.98	0.04	1.30	0.17	1.23	0.12	1.09	0.16	1.11	0.24

Table 3-3 – Overall summary of statistical data for all columns in database

		Columns with Steel Jackets		Columns with FRP Jackets	
		V_y calc/V_y test	$V_{peak\ calc}/V_{peak\ test}$	$V_{y\ calc}/V_{y\ test}$	$V_{peak\ calc}/V_{peak\ test}$
All Circular Specimens	Mean	1.09	1.08	1.38	1.16
	STD	0.14	0.15	0.30	0.23
All Rectangular Specimens	Mean	1.25	1.12	1.56	1.14
	STD	0.35	0.18	0.61	0.20

CHAPTER 4 NON-LINEAR DEFORMATION PARAMETERS OF JACKETED COLUMNS

This chapter presents the procedure that was followed to estimate non-linear deformation parameters for FRP- or steel-jacketed columns. Because of the large variety of testing configurations and retrofitting arrangements, and because of the lack of physical models that describe column lateral deformations laterally, a statistical approach was followed to estimate jacketed column deformations at different levels.

4.1 Histograms and Statistical Properties of Jacketed Columns in Database

The laboratory tests had different arrangements and column sizes, so deformations measured during the tests were normalized by height to obtain drift (Δ/H). The deformation data was then classified by jacketing materials, 84 and 32 columns retrofitted using FRP and steel materials, respectively.

The deformation parameters were studied statistically to determine deformation values for jacketed columns. Some physical constraints had to be applied to the statistical analysis to reflect physical behavior of jacketed columns. The constraints included are:

- Deformations cannot be negative
- Yield deformation is equal or lower than the deformation at peak ($\Delta_y \leq \Delta_p$).
- The maximum deformation cannot exceed a drift of 10%
- The yield deformation should remain below a 2% drift

Figure 4-1 shows histograms of deformations at yield and peak of jacketed columns and the corresponding Parameter a. From these results it can be observed that both jacket materials resulted in similar yield deformations of jacketed columns but notably different values of peak deformation.

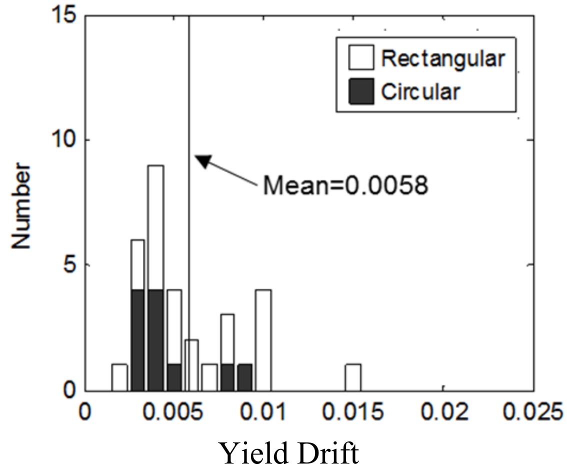

(a) Steel-jacketed columns

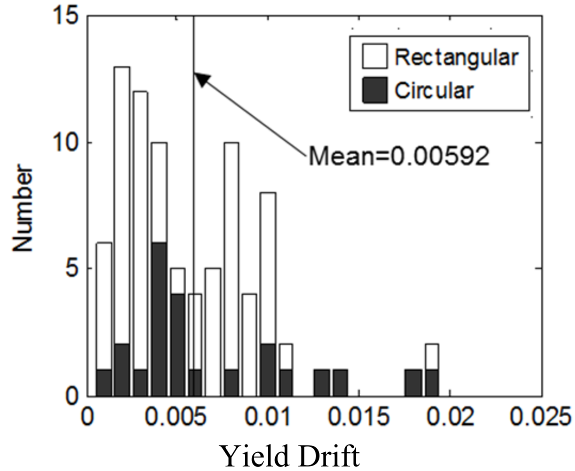

(b) FRP-jacketed columns

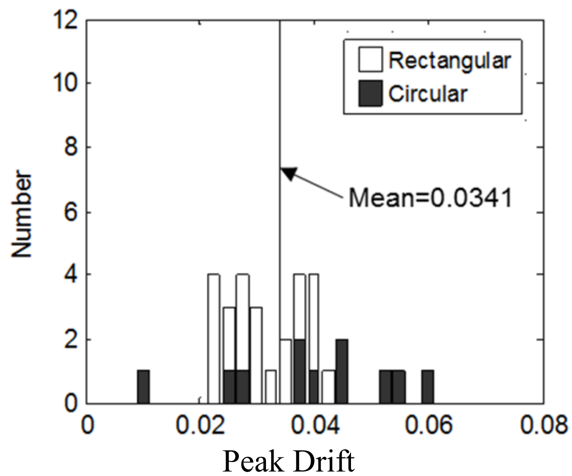

(c) Steel-jacketed columns

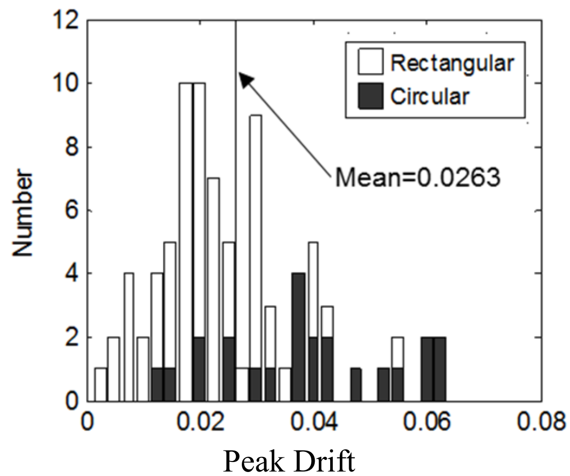

(d) FRP-jacketed columns

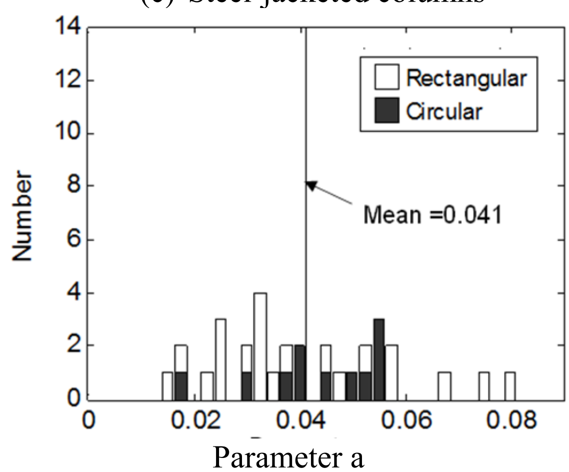

(e) Steel-jacketed columns

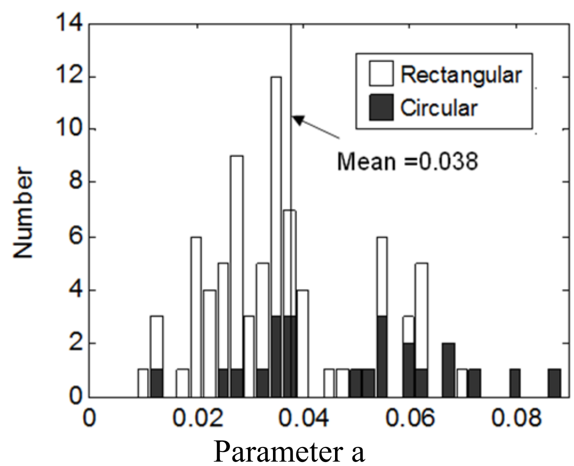

(f) FRP-jacketed columns

Figure 4-1 Histograms from deformations parameters (yield, peak, *a*)

The column database includes both circular and rectangular cross section shapes. Due to the limited amount of experimental data the study explored the possibility of joining the data of the two types of geometries, even though the measured behavior was dissimilar. To evaluate the possibility of studying the data collectively, the statistical properties of deformations from both types of sections must have similar mean values, similar standard deviation (STD) values, and similar cumulative density functions curves. The two-sample Kolmogorov-Smirnov goodness-of-fit hypothesis test (KS test, Benjamin and Cornell 1970) was used to evaluate the two distributions using Eq. 4-12. In Eq. 4-12 $F_{i,n}$ refer to the data i cumulative density functions (CDF) and x is the different values of the data. This test uses the CDF both datasets that are compared and reports with at a prescribed level of confidence whether or not the data CDF have the same distribution (h = 1 to reject the hypothesis and h = 0 to accept the hypothesis for the prescribed level of confidence). The results from these tests were plotted and shown in Figure 4-2.

$$D_{n,n'} = \sup\left|F_{1,n}(x) - F_{2,n'}(x)\right|, x \qquad \textbf{Eq. 4-1}$$

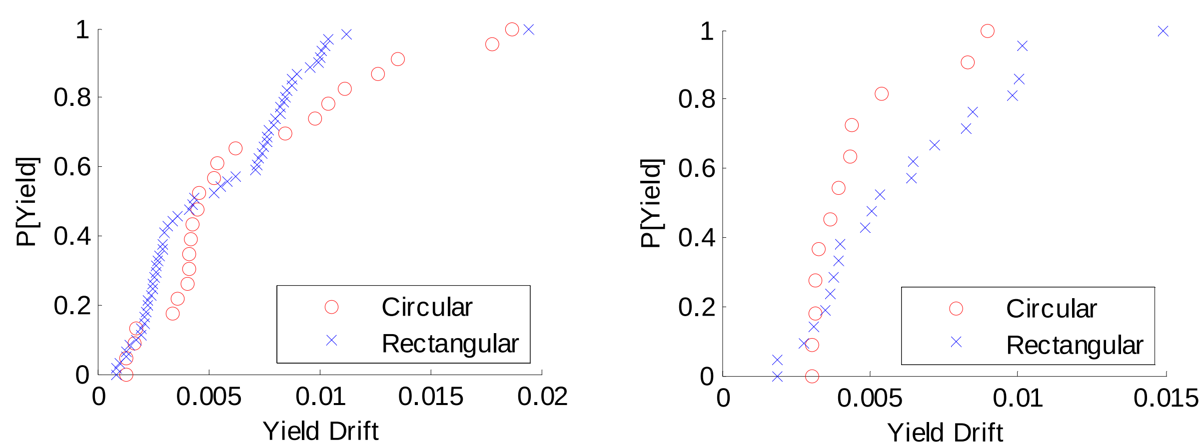

(a) FRP jacketed columns (h = 0) (b) Steel jacketed columns (h = 0)

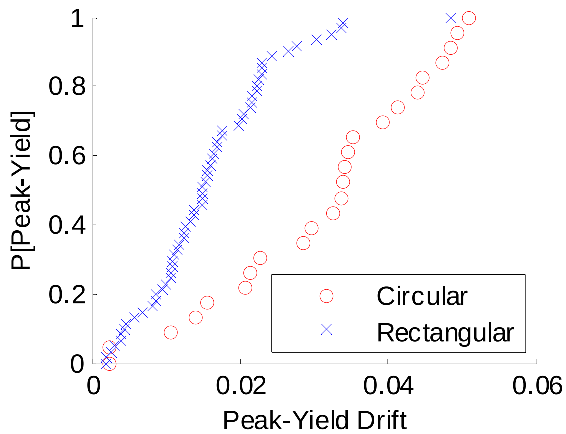

(c) FRP jacketed columns (h = 1)

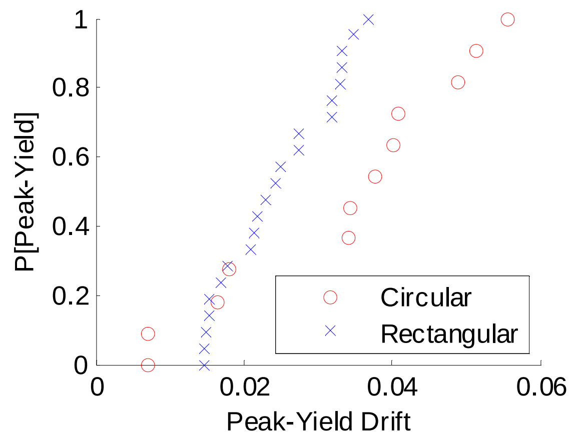

(d) Steel jacketed columns (h = 1)

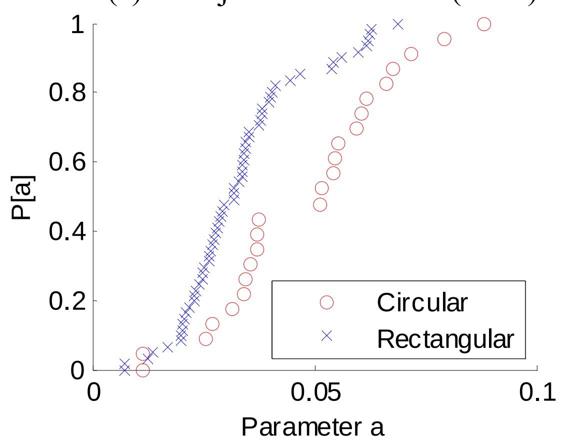

(e) FRP jacketed columns (h = 1)

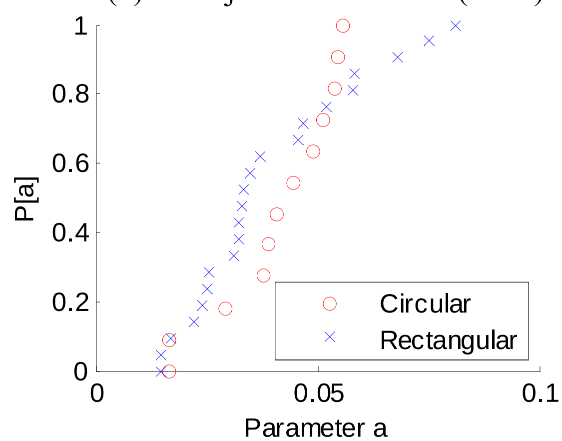

(f) Steel jacketed columns (h = 0)

Figure 4-2 Empirical CDF comparison between circular and rectangular columns retrofitted with steel or FRP

The KS test shown in Figure 4-2 accepted the null hypothesis with a 95% probability for yield deformation of both jacketing materials and *a* parameter for steel jacketed columns while peak to yield deformations and *a* parameter of FRP jacketed columns was rejected at probability values up to 90%. Furthermore, after an additional visual inspection of the CDF at the different deformations levels it was concluded that for yield, the circular and rectangular data can be used together but the other deformations need to be studied separately.

4.2 Matching Data to a Statistical Distribution

Common statistical distributions were matched to the measured drift data to determine probabilities of exceedance. To match statistical distribution both the probability density function (PDF) and cumulative density function (CDF) were used to match the data visually.

The following 3 statistical distributions were tested (Boucher 2009):

1. Log-Normal - $Fx(x; \mu, s) = \Phi\left(\frac{\ln(x-\mu)}{s}\right)$ for $x > 0$

2. Weibull - $Fx(x; k, \mu) = 1 - e^{-\left(\frac{x}{\mu}\right)^k}$ for $x \geq 0$ if $x < 0$ then $Fx(x; k, \mu) = 0$

3. Rayleigh - $Fx(x; \mu) = 1 - e^{-\frac{x^2}{2\mu^2}}$ for $x \geq 0$

Only the statistical distributions listed above satisfy the physical constraints mentioned earlier. The different distribution fitting parameters relate the data to these distributions. The log-normal statistical distribution has two fitting parameters: the mean (μ) and the parameter "s" related to the standard deviation of the normal distribution. The Weibull distribution has two fitting parameters, which are called shape factors: *k* is a shape parameter for the distribution and μ is a scaling parameter for the statistical distribution. The Rayleigh distribution, also known as one parameter Weibull distribution, follows the same equation as the Weibull distribution but with the shape parameter *k* set equal to 2. The statistical parameters required in each distribution were obtained using MATLAB & Simulink predefined functions. To compare the distributions the calculated parameters were used to plot the estimated distributions with the empirical data. The process was followed for the Log-normal, Weibull and Rayleigh distribution for all deformations. Figure 4-3 shows all the parameters with the estimated distributions.

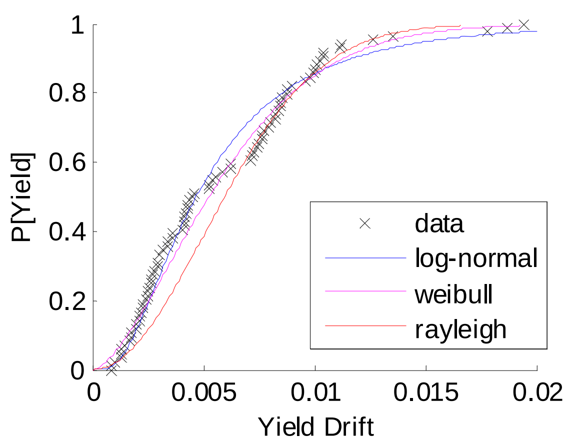

(a) FRP-jacketed columns

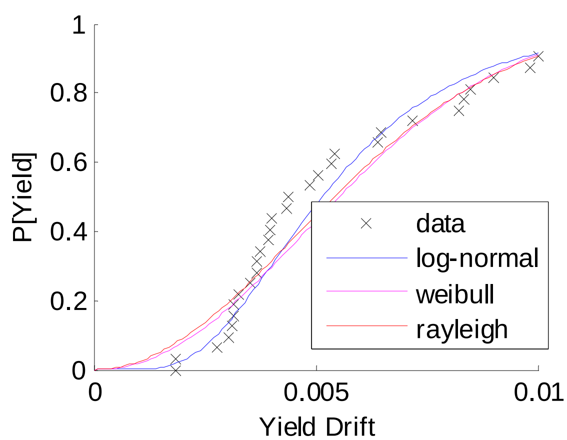

(b) Steel-jacketed columns

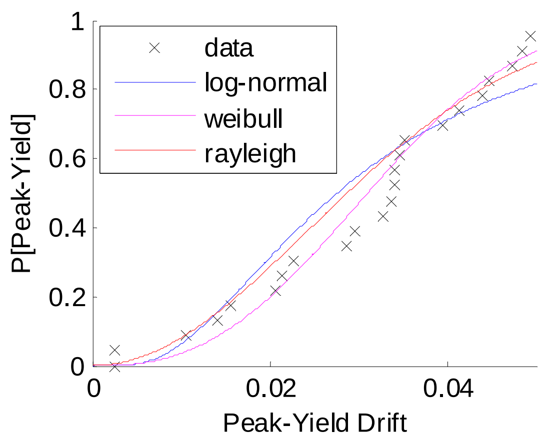

(c) Circular FRP-jacketed columns

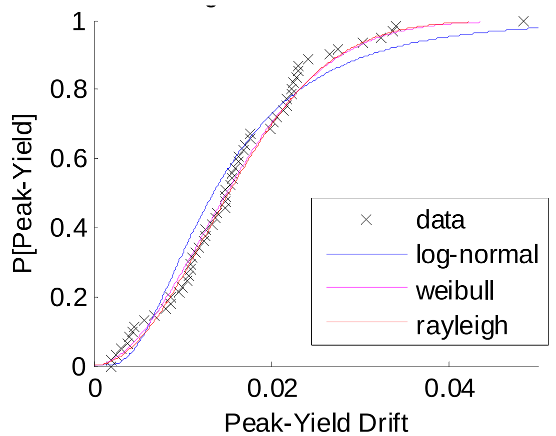

(d) Rectangular FRP-jacketed columns

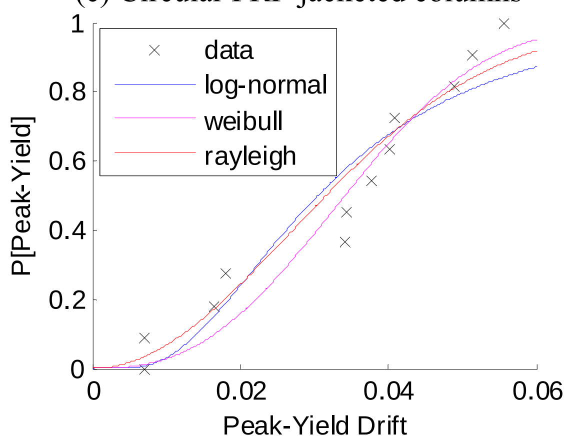

(e) Circular Steel-jacketed columns

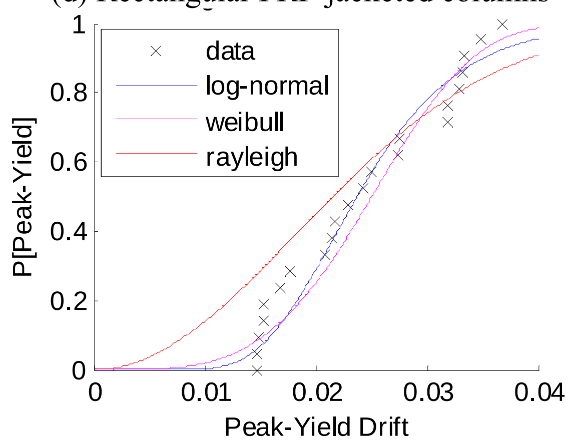

(f) Rectangular Steel-jacketed columns

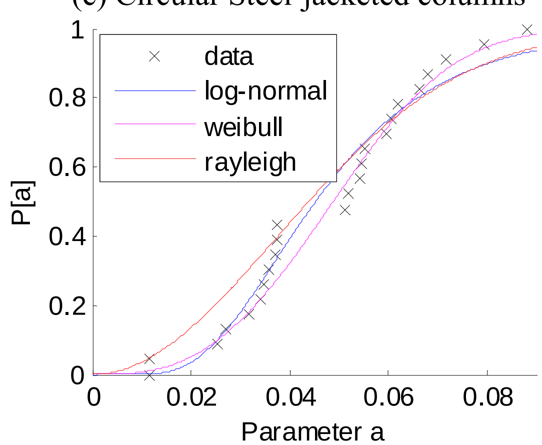

(g) Circular FRP-jacketed columns

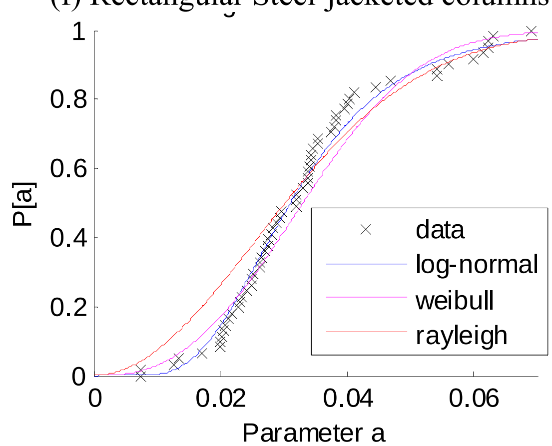

(h) Rectangular FRP-jacketed columns

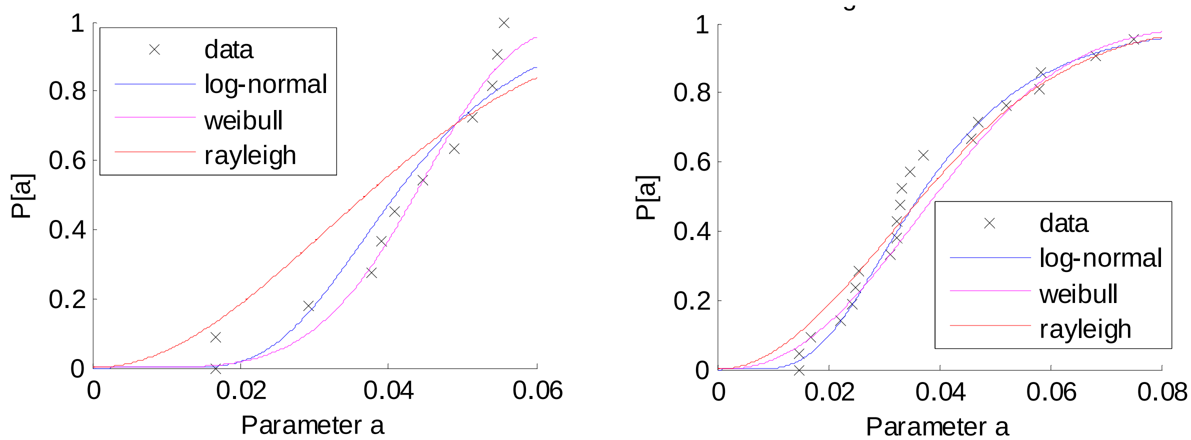

(i) Circular Steel-jacketed columns (j) Rectangular Steel-jacketed columns

Figure 4-3 Distribution comparisons with a values data

After observing individual figures that compared the different data to the distributions, it was determined that the Weibull distribution gave a better approximation for all deformations (final distributions are shown in Figure 4-4). Using the distributions, the deformation values for columns for a desired probability of exceedance could be determined.

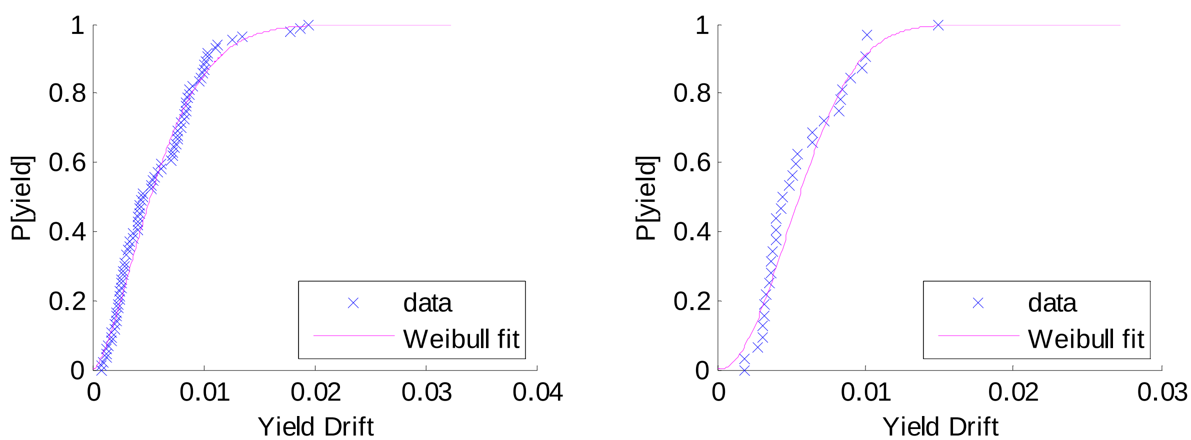

(a) FRP-jacketed columns (b) Steel-jacketed columns

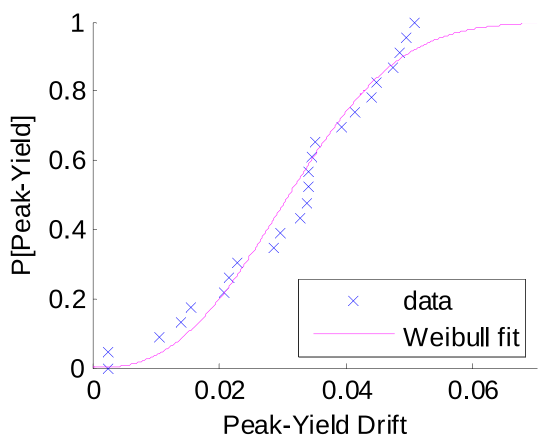

(c) Circular FRP-jacketed columns

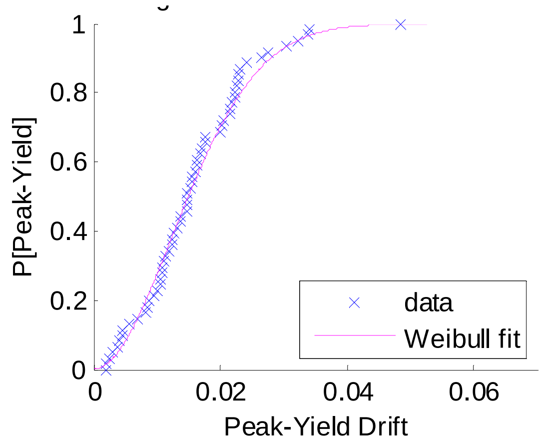

(d) Rectangular FRP-jacketed columns

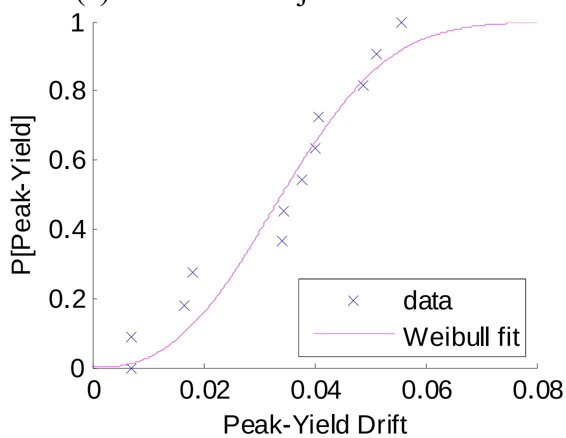

(e) Circular Steel-jacketed columns

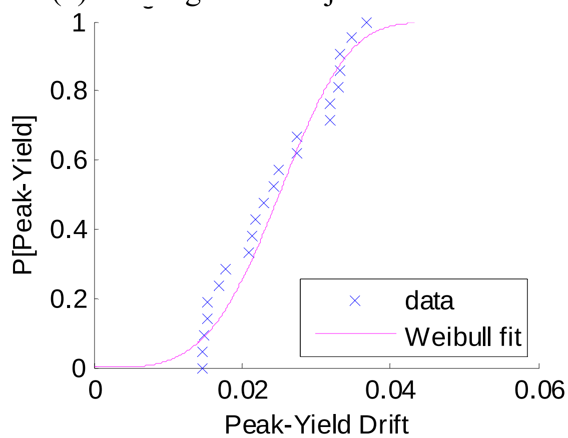

(f) Rectangular Steel-jacketed columns

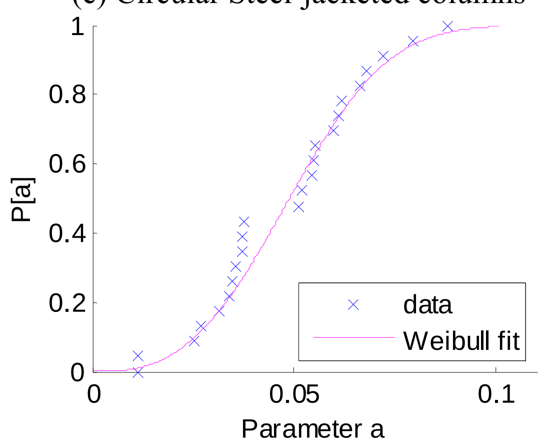

(c) Circular FRP-jacketed columns

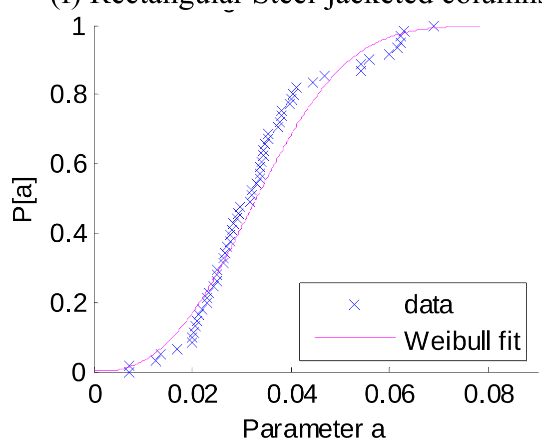

(d) Rectangular FRP-jacketed columns

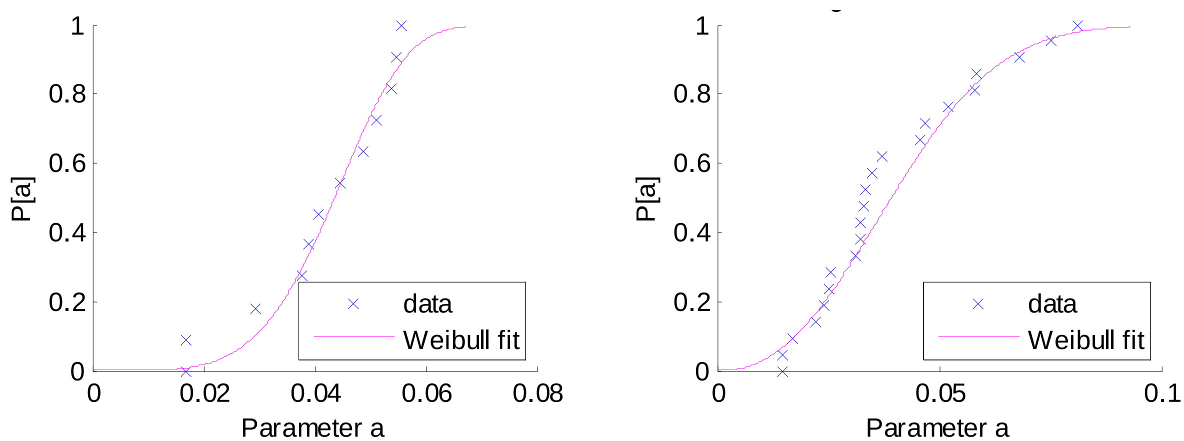

(e) Circular Steel-jacketed columns (f) Rectangular Steel-jacketed columns

Figure 4-4 Empirical data cdf with the final distributions

The fitting values for the Weibull distribution of each column shape and jacketing material are listed in Table 4-1. The fitting values were obtained using maximum likelihood estimates which were obtained following a process similar to the one described by Clifford (1965).

Table 4-1 Fitting parameters for Weibull distribution at the different deformation levels

			μ	k
FRP	Δ_y	Circular	0.0066	1.57
		Rectangular		
Steel	Δ_y	Circular	0.0066	2.10
		Rectangular		
FRP	$\Delta_p - \Delta_y$	Circular	0.0357	2.61
		Rectangular	0.0181	1.91
Steel	$\Delta_p - \Delta_y$	Circular	0.0393	2.61
		Rectangular	0.0275	3.89
FRP	a	Circular	0.0553	2.91
		Rectangular	0.0380	2.64
Steel	a	Circular	0.0471	4.74
		Rectangular	0.0458	2.36

4.3 Drifts Determined from Selected Statistical Distributions

The distributions give the deformations at different probabilities. From the distributions the probability of exceedance was calculated. The probability of exceedance was calculated using Eq. 4-14. The probability of exceedance shows the probability of the selected parameter reaching the target value. Some of these values are shown in Table 4-2).

$$\text{Probability of exceedance} = (1 - P[x]) * 100 \qquad \textbf{Eq. 4-2}$$

Table 4-2 Deformation parameters at different levels of probability

Probability of Exceedance	FRP		Steel	
	a		*a*	
	Circular	Rectangular	Circular	Rectangular
95	0.0199	0.0123	0.0251	0.0130
90	0.0255	0.0161	0.0293	0.0176
85	0.0296	0.0190	0.0321	0.0212
80	0.0330	0.0214	0.0343	0.0242
75	0.0360	0.0236	0.0362	0.0270
70	0.0388	0.0256	0.0379	0.0295
65	0.0414	0.0275	0.0394	0.0320
60	0.0439	0.0294	0.0408	0.0344
55	0.0463	0.0312	0.0422	0.0368
50	0.0487	0.0330	0.0436	0.0392

4.4 Recommended Plastic Deformation Values (Parameter *a*) for Jacketed Columns

Using the statistical data developed in this research for both circular and rectangular jacketed columns, respectively, modeling parameters for drift of jacketed columns are proposed following the format of *ACI 369R-11* and *ASCE/SEI 41-06* (Parameters *a* and *b*). The proposed modeling parameters are separated by jacketing material and cross section geometry since the statistical study revealed differences in drift values within each of these groups. Table 4-3 lists the proposed values of drift Parameters *a* and *b*.

Table 4-3 Proposed modeling parameters for FRP- and steel-jacketed columns

Section Parameters			Modeling parameters		
			Plastic rotations angle, radians		Residual Strength ratio
Jacketing Material	Section Shape	$\frac{P}{A_g f_c'}$	a	b	C
FRP	Circular	≤ 0.1	0.049	0.060	0.2
		≥ 0.6	0.010	0.010	0.0
	Rectangular	≤ 0.1	0.034	0.060	0.2
		≥ 0.6	0.010	0.010	0.0
Steel	Circular	≤ 0.1	0.043	0.060	0.2
		≥ 0.6	0.010	0.010	0.0
	Rectangular	≤ 0.1	0.040	0.060	0.2
		≥ 0.6	0.010	0.010	0.0

Only Parameter a was determined statistically in this research because of limited experimental data to calculate Parameter b. It is recommended, therefore, that Parameter b be the one proposed for existing columns with transverse reinforcement ratio, $\rho_v \geq 0.006$, until further data are available from laboratory experiments of jacketed columns tested to reach column strength degradation past 20%. The study published by Ghosh (2007) was one of the few tests where the researcher recorded drifts corresponding to high strength degradation of the jacketed column specimens. Ghosh (2007) studied reinforced concrete columns with short lap-splices retrofitted with FRP jackets. These columns were subjected to quasi-static cyclic loading and in some cases reached the rupture of the jacket and strength degradation up to 90%. From that study the hysteretic curves exhibited show a gradual degradation of strength as lateral deformation increased, as well as decreased pinching and high levels of plasticity reaching values of parameter b of 0.11. This value significantly exceeds the largest Parameter b value for existing columns in *ACI 369R-11*.

The recommended values of Parameters b and c are based in the similarities observed in the behavior of jacketed columns in comparison with columns containing reinforcing details representative of new design (code conforming columns). The similarities in backbone behavior of an originally deficient column that has been retrofitted using two different jacketing configurations with the behavior of a similar code-conforming column is shown in **Figure 4-5**.

The behavior of the jacketed columns is remarkably similar to that of columns with well detailed reinforcement, providing support for using modeling parameters of these columns for jacketed columns where there are no available laboratory data.

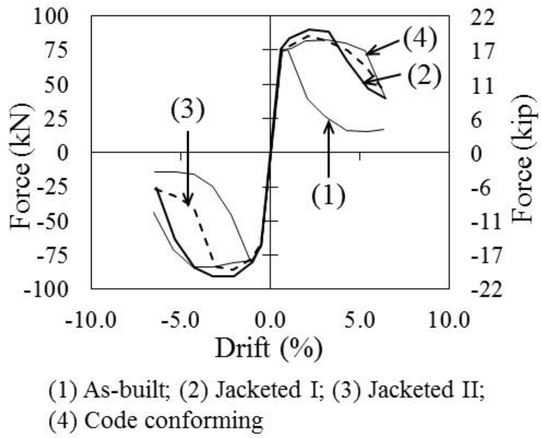

Figure 4-5 Comparison of the backbone force-deformation behavior of a code-conforming and two different jacketed columns

CHAPTER 5 SUMMARY AND CONCLUSIONS

This research concentrated on determining nonlinear modeling parameters for jacketed reinforced concrete columns based on behavior measured during laboratory tests. The jacketing materials studied included either fiber reinforced polymers (FRP) or steel. By eliminating detailing and design deficiencies of existing columns, jacketing increases displacement ductility, stiffness and strength while largely maintaining the original column dimensions. The laboratory experiments used in this research included columns with different amounts of longitudinal steel reinforcement, column geometry and loading protocols. The test details were meant to capture three types of reinforced column deficiencies: low shear strength, insufficient confinement of the concrete core and short lap-splices within the plastic hinge regions.

A database of jacketed columns was assembled to study the behavior of these elements under quasi-static lateral loading. A procedure to calculate yield and peak strength of jacketed columns is discussed in Chapter 3. The lateral deformation capacity (drift) of jacketed columns was determined using a statistical study as discussed in Chapter 4.

5.1 Characterization of Jacketed Column Behavior

The study of a database of jacketed columns revealed that jacketing eliminated the potential for shear failure within the jacketed region and the section would be flexure dominated. The flexural strength of a jacketed column can then be estimated using a fiber model. The fiber model must include the confining effect of the jacket on the concrete. Using this procedure, the jacketed column strength (yield and peak) was estimated within approximately ±10%.

Plastic drift capacity was estimated using a statistical study. The drift capacity of circular jacketed columns is significantly different from that of rectangular jacketed columns. Therefore jacketed column deformations were studied separately as a function of column geometry. The type of jacket (FRP or steel) also affected the calculated drift capacities so columns were also separated according to jacket type. A Weibull statistical distribution best described the distribution of Parameter *a* found in columns from the jacketed column database. A proposed set of modeling parameters for drift (Parameters *a* and *b*) were proposed on this study; Parameter *c* that represents the residual column strength at large deformations was proposed to be 0.2 times the peak strength as is commonly used for existing columns.

CHAPTER 6 REFERENCES

Aboutaha, R. S., Engelhardt, M. D., Jirsa, J. O., and Kreger, M. E.. "Rehabilitation of Shear Critical Concrete Columns by Use of Rectangular Steel Jackets". *ACI Structural Journal*. V. 96, No. 1, 1999, pp. 68-78.

Aboutaha, R. S., Engelhardt, M. D., Jirsa, J. O., and Kreger, M. E.. "Retrofit of Concrete Columns with Inadequate Lap Splices by the Use of Rectangular Steel Jackets". *Earthquake Spectra*, V. 12, No. 4, 1996, pp. 693-714.

Aboutaha, R. S., Engelhardt, M. D., Jirsa, J. O., & Kreger, M. E.. "Experimental Investigation of Seismic Repair of Lap Splice Failures in Damaged Concrete Columns". *ACI Structural Journal*, V. 96, No. 2, 1999, pp. 297-307.

ACI Committee 369. 2011. "Guide for Seismic Rehabilitation of Existing Concrete Frame Buildings", ACI 369R-11, *American Concrete Institute*, Farmington Hills, MI.

ACI Committee 440. 2008. "Guide for the Design and Construction of Externally Bonded FRP Systems for Strengthening Concrete Structures". ACI 440.2R-08, *American Concrete Institute*, Farmington Hills, MI.

Alcocer, S. M., and Durán-Hernández, R. "Seismic Performance of a RC Building with Columns Rehabilitated with Steel Angles and Straps. Innovations in Design with Emphasis on Seismic, Wind, and Environmental Loading". Quality Control and Innovations in Materials/Hot Weather Concreting. 2002, pp. 531-552.

Alvarez, J. C., & Brena, S. F.. "Non-linear Modeling Parameters for Jacketed Columns Used in Seismic Rehabilitation of RC Buildings". *ACI Special Publication*, 2014, SP297-6

ASCE. 2006. "Seismic Rehabilitation of Existing Buildings", ASCE/SEI 41-06, American Society of Civil Engineers, Reston, VA.

Breña, S. F., and Schlick, B. M.. "Hysteretic Behavior of Bridge Columns with FRP-Jacketed Lap Splices Designed for Moderate Ductility Enhancement".*Journal of Composites for Construction.* V. 11, No. 6, 2007, pp. 565-574.

Bucher, C., 2009. "Computational Analysis of Randomness in Structural Mechanics". *Structures and Infrastructures Book Series* . V. 3. CRC Press.

Chai, Y. H., Nigel Priestley, M. J. N., Seible, F., California., and University of California, San Diego.. "Seismic Retrofit of Circular Bridge Columns for Enhanced Flexural Performance". *ACI Structural Journal*, V. 88, No. 5, 1991, pp. 572-584.

Cho, J.-Y., and Pincheira, J. A., “Inelastic Analysis of Reinforced Concrete Columns with Short Lap Splices Subjected to Reversed Cyclic Loads,” *ACI Structural Journal*, V. 103, No. 2, 2006, pp. 280-290.

Ciampi, V., MA Crisfield, Non-linear Finite Element Analysis of Solids and Structures. *Meccanica*, V. 32, No. 6, 1997, pp.586-587.

Cook, R. D. (2007). “Concepts and applications of finite element analysis”. John Wiley & Sons.

Esmaeily, A., and Xiao, Y.. “Seismic Behavior of Bridge Columns Subjected to Various Loading Patterns”. California: *Pacific Earthquake Engineering Research Center* (PEER), 2002/15.

Esmaeily, A., and Xiao, Y.. “Behavior of Reinforced Concrete Columns Under Variable Axial Loads: Analysis”. *ACI Structural Journal*, V. 102, No. 5, 2005, pp. 736-744.

Galal, K., Arafa, A., and Ghobarah, A.. "Retrofit of RC Square Short Columns". *Engineering Structures*. V. 27, No. 5, 2005, pp. 801-813.

Ghosh, K. K., & Sheikh, S. A.. “Seismic upgrade with carbon fiber-reinforced polymer of columns containing lap-spliced reinforcing bars.” *ACI Structural Journal*, V. 104, No. 2, 2007, pp. 227-236

Harajli, M. H.. "Behavior of Gravity Load-Designed Rectangular Concrete Columns Confined with Fiber Reinforced Polymer Sheets". *Journal of Composites for Construction*. V. 9, No. 1, 2005, pp. 4-14.

Harajli, M. H., and Rteil, A. A.. "Effect of Confinement Using Fiber-Reinforced Polymer or Fiber-Reinforced Concrete on Seismic Performance of Gravity Load-Designed Columns". *ACI Structural Journal*. V. 101, No. 1, 2004, pp. 47-56.

Harajli M.H., and Dagher F.. "Seismic Strengthening of Bond-Critical Regions in Rectangular Reinforced Concrete Columns Using Fiber-Reinforced Polymer Wraps". *ACI Structural Journal*. V. 105, No. 1, 2008, pp. 68-77.

Harries, K. A., Ricles, J. R., Pessiki, S., & Sause, R.. “Seismic retrofit of lap splices in nonductile square columns using carbon fiber-reinforced jackets”. *ACI Structural Journal*, V. 103, No. 6, 2006.

Haroun, M. A., and Elsanadedy, H. M.. "Fiber-Reinforced Plastic Jackets for Ductility Enhancement of Reinforced Concrete Bridge Columns with Poor Lap-Splice Detailing". *Journal of Bridge Engineering*. V. 10, No. 6, 2005, pp. 749-757.

Haroun, M. A., and Elsanadedy, H. M.. "Behavior of Cyclically Loaded Squat Reinforced Concrete Bridge Columns Upgraded with Advanced Composite-Material Jackets". *Journal of Bridge Engineering*. V. 10, No. 6, 2005, pp. 741-748.

Hwang, J.-S., Li, Y.-F., Chen, S.-H., and Hsieh, Y.-M.. "A Study of Reinforced Concrete Bridge Columns Retrofitted by Steel Jackets". *Journal of the Chinese Institute of Engineers*, V. 28, No. 2, 2005, pp. 319-328.

Hoshikuma, J., K. Kawashima, K. Nagaya, and A. W. Taylor. "Stress-Strain Model for Confined Reinforced Concrete in Bridge Piers". *Journal of Structural Engineering* V.123, No. 5, 1997, pp. 624-633.

Iacobucci, R. D., Sheikh, S. A., and Bayrak, O.. "Retrofit of Square Concrete Columns with Carbon Fiber-Reinforced Polymer for Seismic Resistance". *ACI Structural Journal*. V. 100, No. 6, 2003, pp. 785-794.

Lam, L., and Teng, J.. "Design-Oriented Stress- Strain Model for FRP-Confined Concrete," *Construction and Building Materials*, V. 17, 2003a, pp. 471-489.

Lam, L., and Teng, J.. "Design-Oriented Stress- Strain Model for FRP-Confined Concrete in Rectangular Columns," *Journal of Reinforced Plastics and Composites*, V. 22, No. 13, 2003b, pp. 1149-1186.

Mander, J. B., Nigel Priestley, M. J., and Park, R.. "Theoretical Stress-Strain Model for Confined Concrete". *Journal of Structural Engineering*, V. 114, No. 8, pp. 1804-1826.

Memon, M. S., and Sheikh, S. A. 2005. "Seismic Resistance of Square Concrete Columns Retrofitted with Glass Fiber-Reinforced Polymer". *ACI Structural Journal*, V. 102, no. 5, 1988, pp. 774-783.

Ozcan, O., Binici, B., & Ozcebe, G.. "Seismic strengthening of rectangular reinforced concrete columns using fiber reinforced polymers". *Engineering Structures*, V. 32 No. 4, 2010, pp. 964-973.

Pekelnicky, R., & Poland, C. 2013. ASCE 41-13: "Seismic Evaluation and Retrofit of Existing Buildings", *SEAOC 2012 Convention Proceedings*, 2012.

Priestley, M.J.N., Seible, F. Xiao, Y., and Verma, R.. "Steel Jacket Retrofitting of Reinforced Concrete Bridge Columns for Enhanced Shear Strength – Part 1: Theoretical Considerations and Test Design." *ACI Structural Journal*, V. 91, No. 4, 1994, pp. 394-405.

Priestley, M. J.N., Seible, F., Xiao, Y., and Verma, R.. "Steel Jacket Retrofitting of Reinforced Concrete Bridge Columns for Enhanced Shear Strength Part 2: Test Results and Comparison with Theory". *ACI Structural Journal*, V. 91, No. 5, 1994, pp. 537-551.

Seible, F., Priestley, M. J. N., Hegemier, G. A., and Innamorato, D.. "Seismic Retrofit of RC Columns with Continuous Carbon Fiber Jackets". *Journal of Composites for Construction*. V. 1, No. 2, 1997, pp. 52-62.

Sezen, H. and Setzler, E. J.. “Reinforcement Slip in Reinforced Concrete Columns”. *ACI Struuctural Journal*, V. 105, No. 3, 2008, pp. 280-289.

Wu, Y.-F., Wang, L., and Liu, T.. "Experimental Investigation on Seismic Retrofitting of Square RC Columns by Carbon FRP Sheet Confinement Combined with Transverse Short Glass FRP Bars in Bored Holes". *Journal of Composites for Construction*. V. 12, No. 1, 2008, pp. 53-60.

Xiao, Y., and Wu., H.. "Retrofit of Reinforced Concrete Columns Using Partially Stiffened Steel Jackets". *Journal of Structural Engineering*. V. 129, No. 6, 2003, pp. 725-732.

Xiao, Y., and Ma, R.. "Seismic Retrofit of RC Circular Columns Using Prefabricated Composite Jacketing". *Journal of Structural Engineering*. V. 123, No. 10, 1997, pp. 1357-1364.

Youm, K.-S., Lee, H.-E., and Choi, S.. "Seismic Performance of Repaired RC Columns". *Magazine of Concrete Research*. V. 58, No. 5, 2006, pp. 267-276.

APPENDIX A: Force-Deformation Envelopes of Columns in Database

Fiber Reinforced Polymer Jacketed Reinforced Concrete Columns Backbones

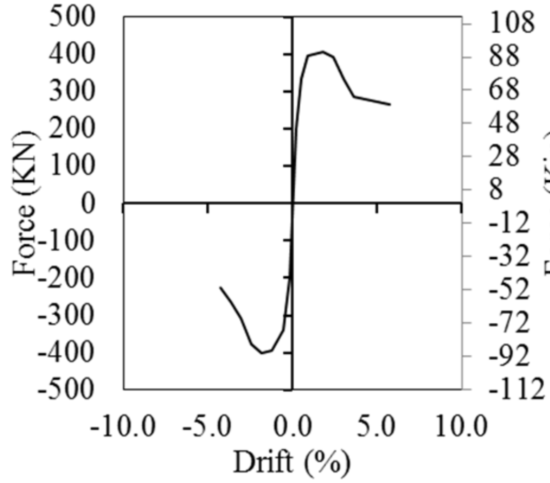

SC1R

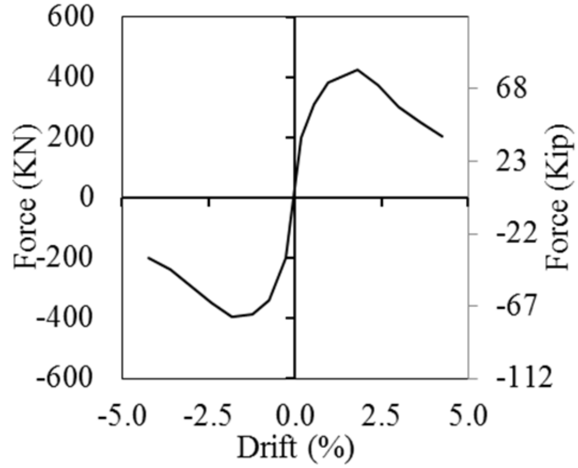

SC2R

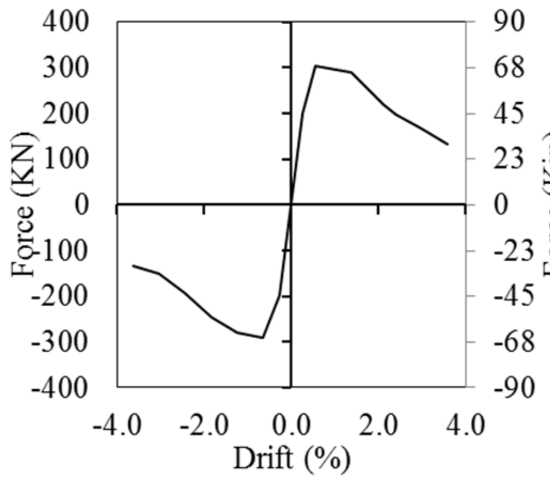

SC2R

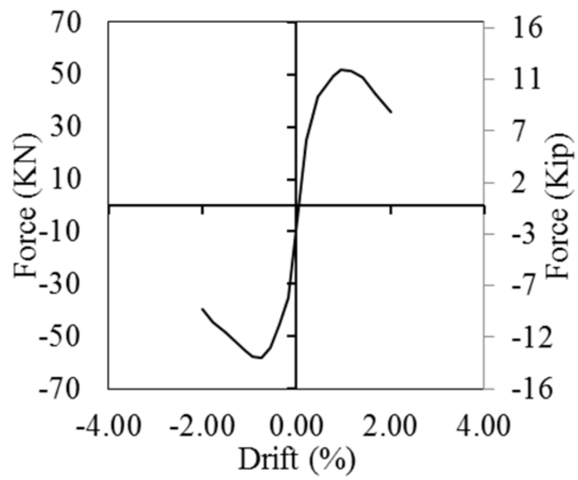

S1

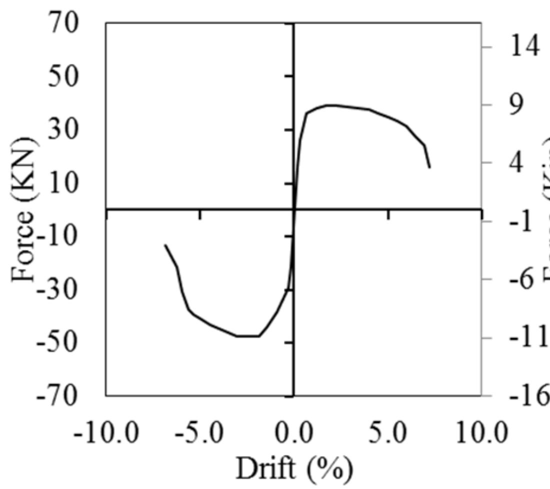

S2

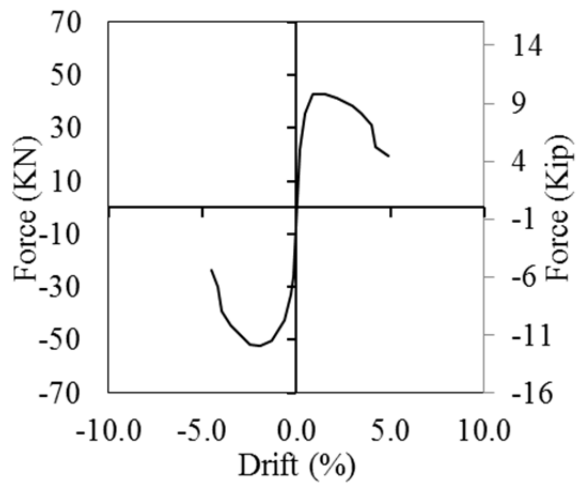

S3

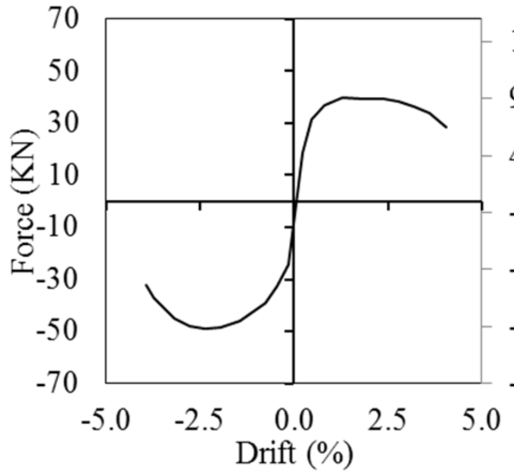

S4

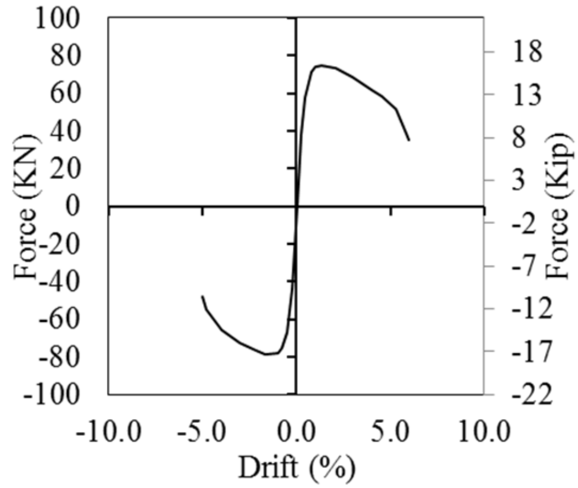

S5

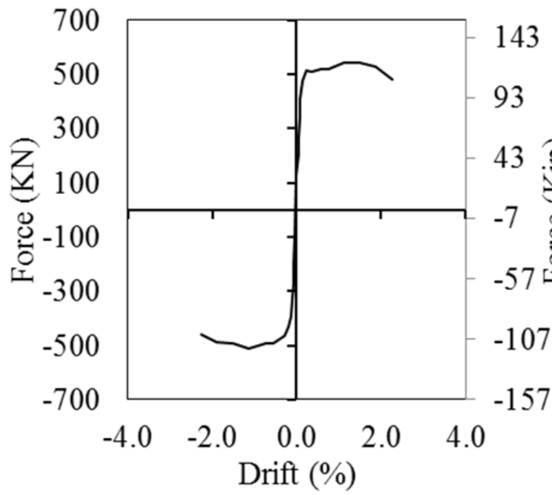

Shear R

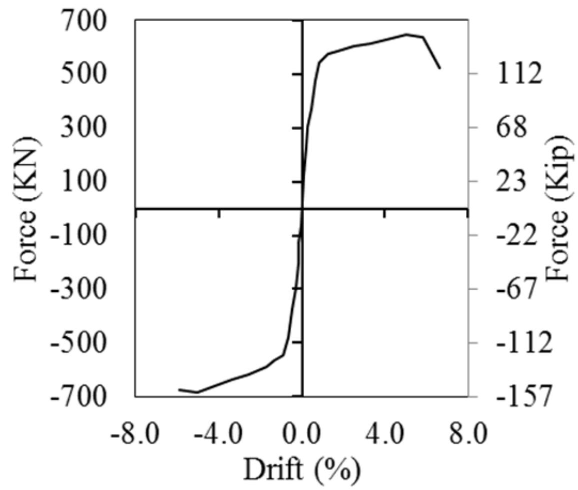

Confinement R

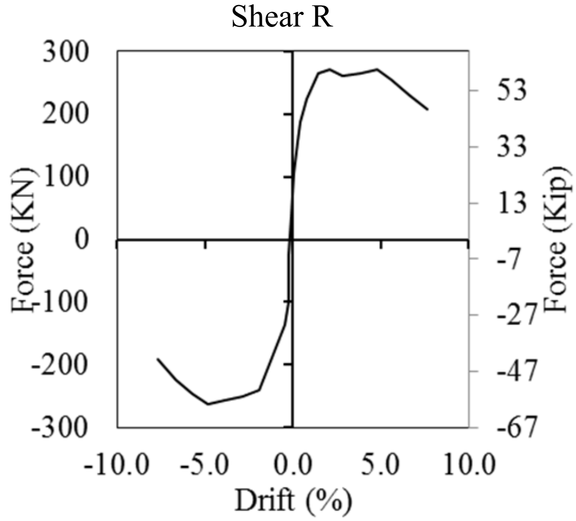

Lap Splice R

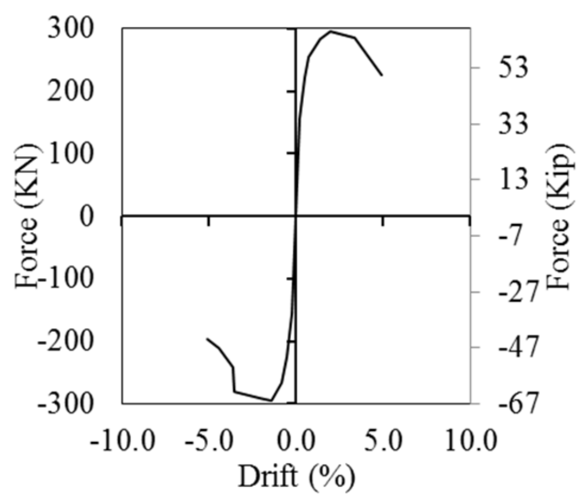

C2

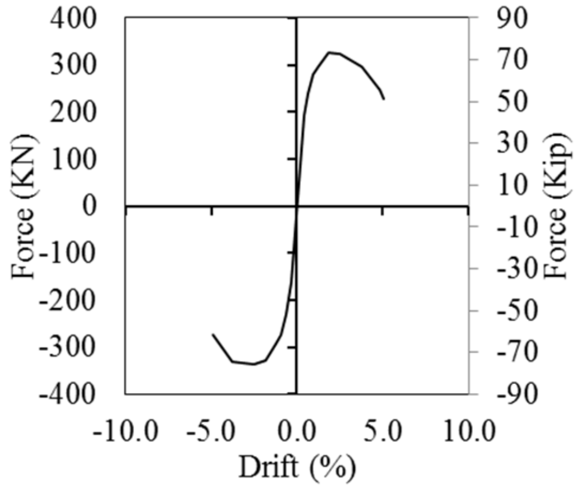

C3

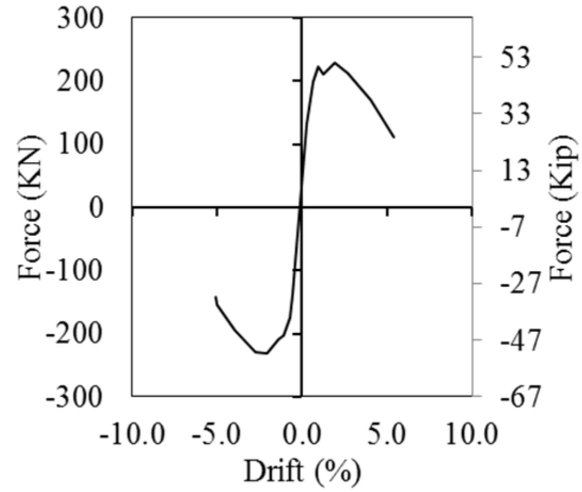

C4

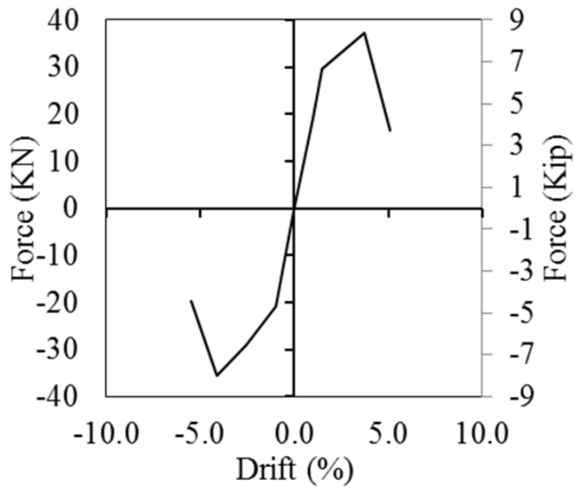

C5

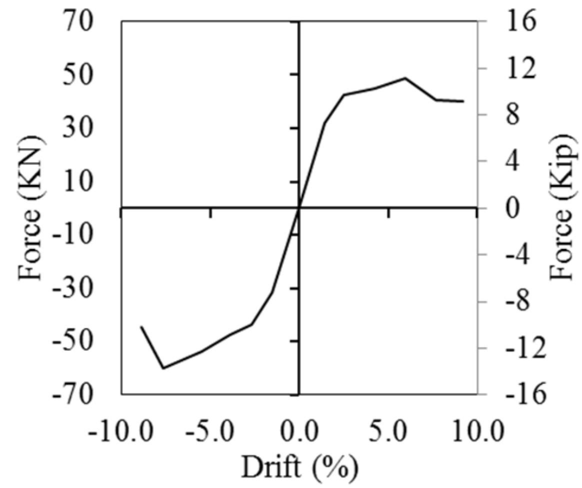

CFRP-05

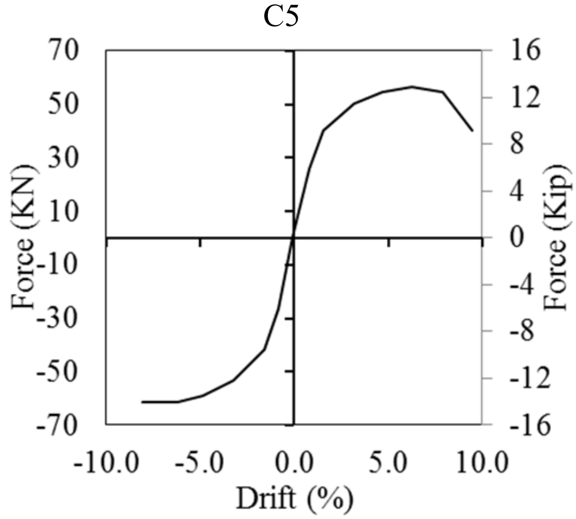

KFRP-05

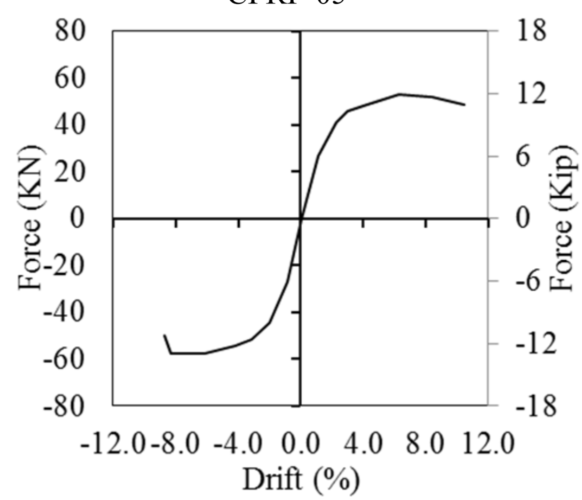

CFRP-15

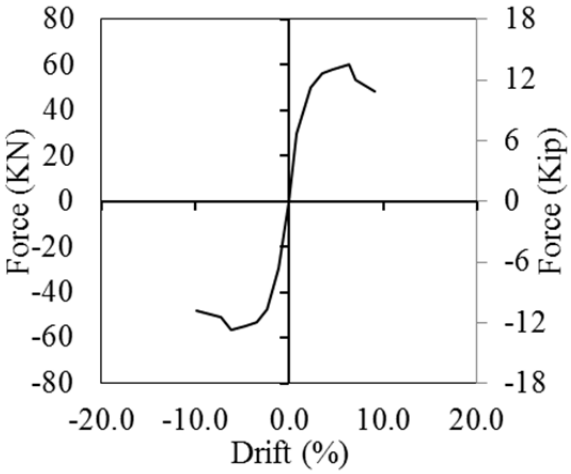

KFRP-15

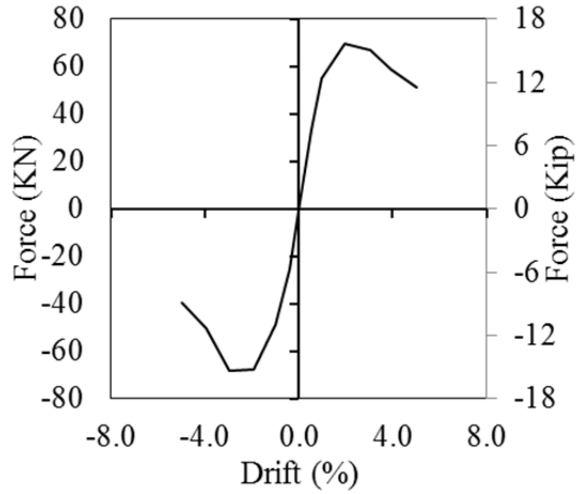

C1-F1

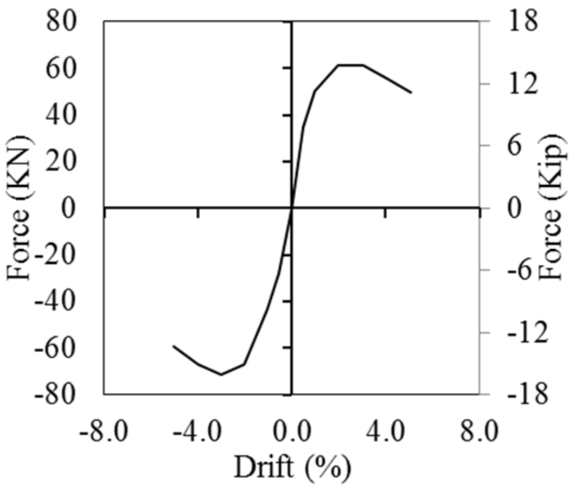

C1-F2

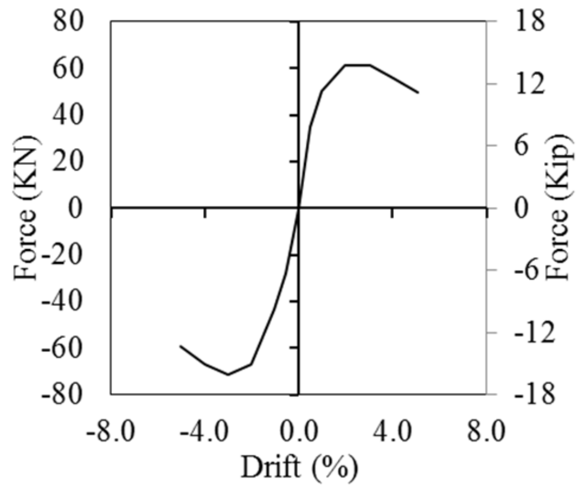

C1-FP1

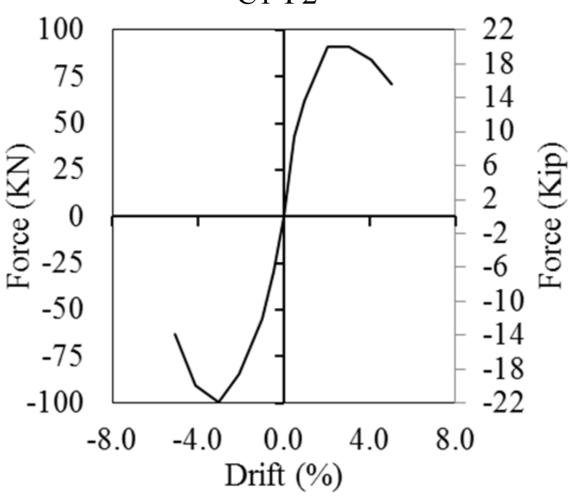

C2-F1

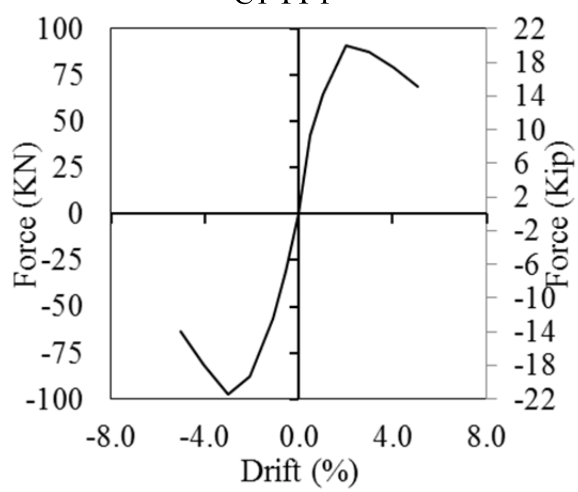

C2-F2

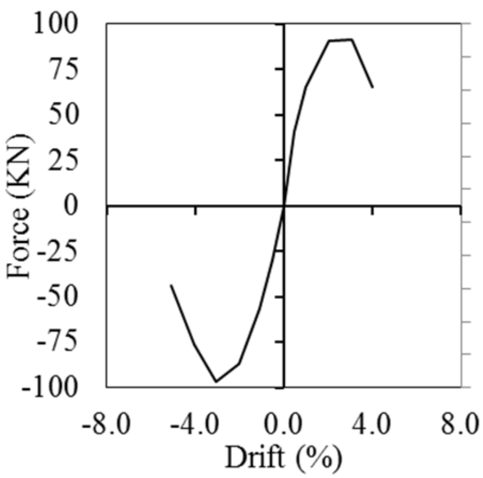

C2-FP1

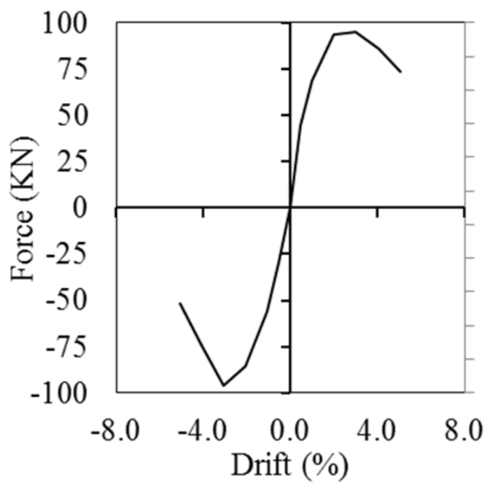

C2-FP2

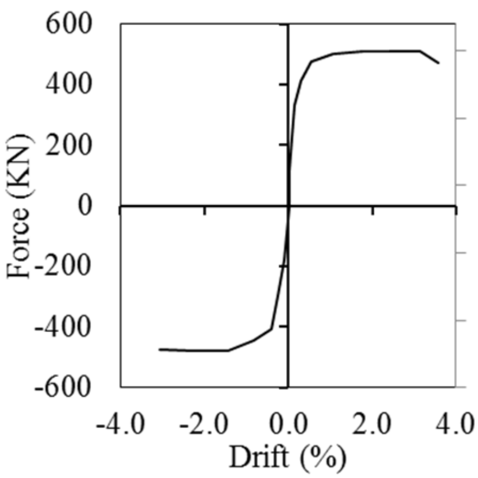

CS-R1

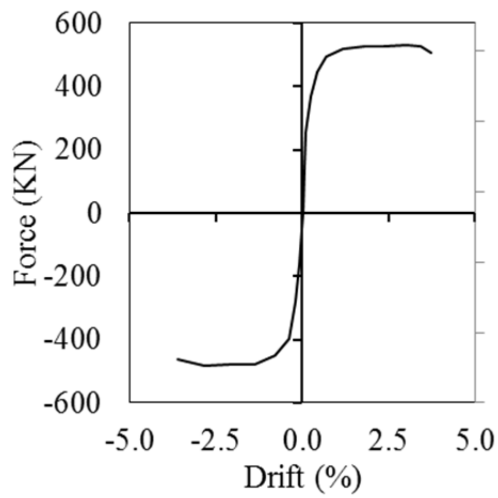

CS-R2

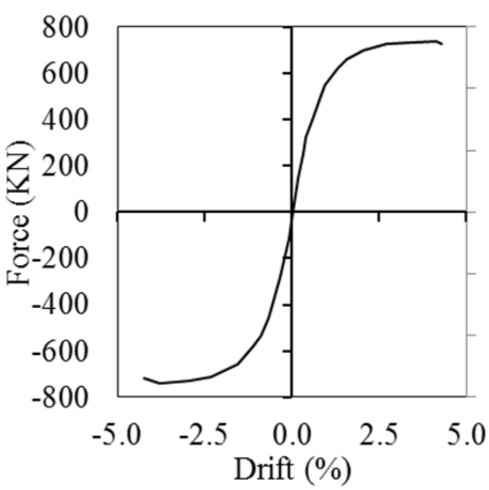

CS-R3

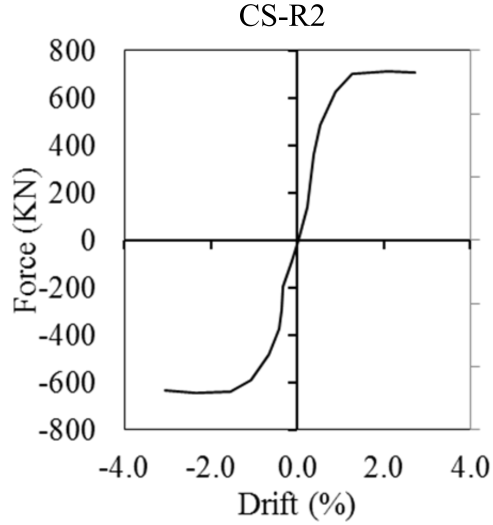

CS-R4

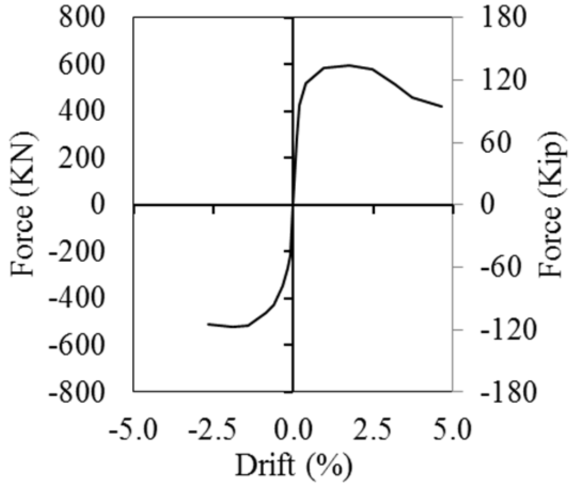

RS-R1

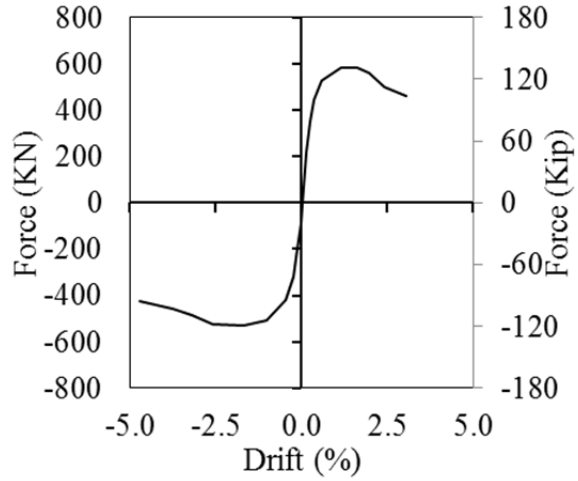

R2-R2

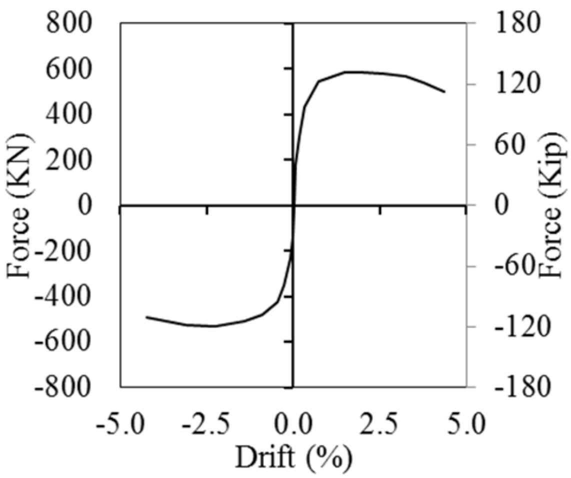

RS-R3

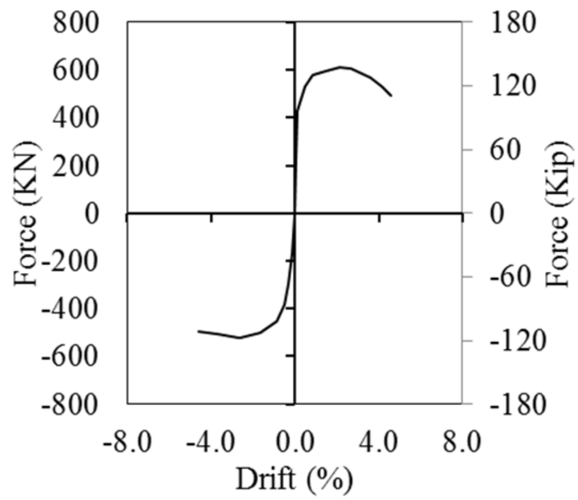

RS-R4

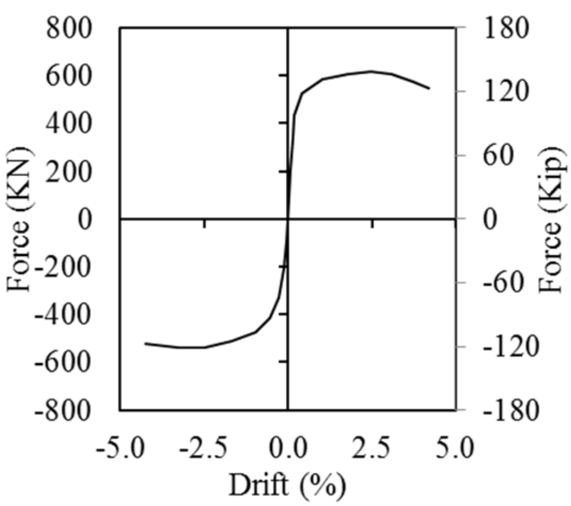

RS-R5

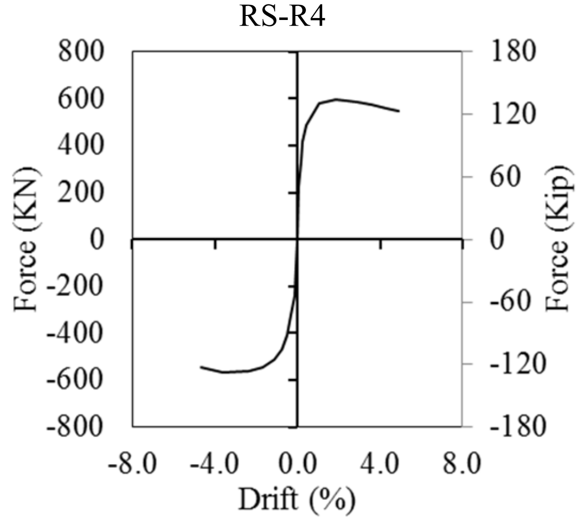

RS-R6

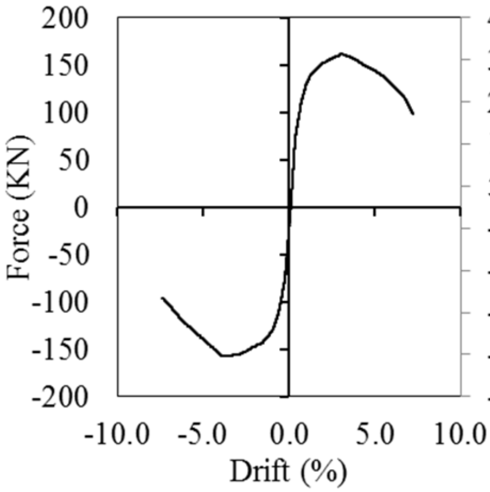

CF-R1

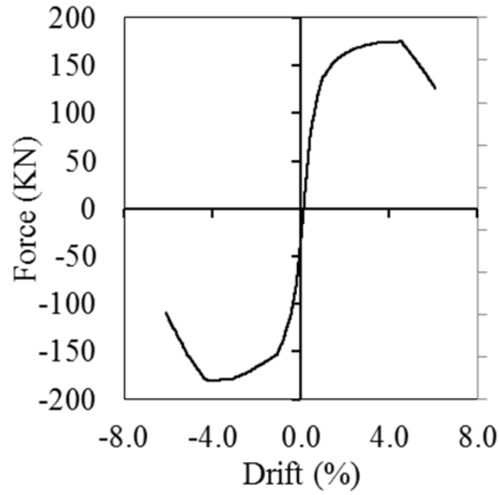

CF-R2

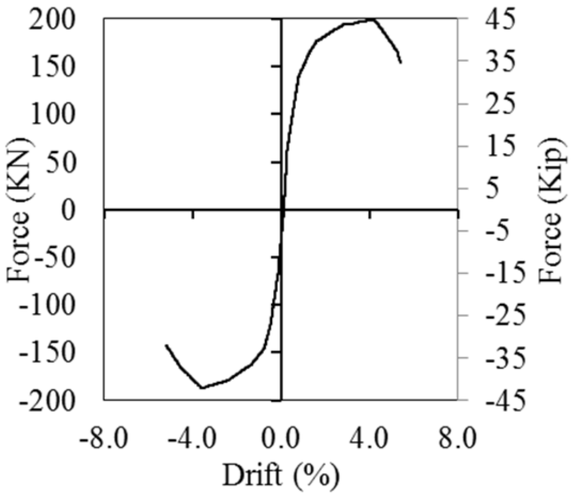

CF-R3

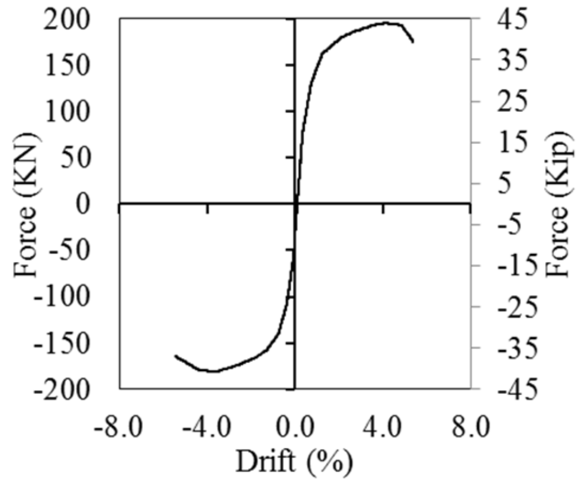

CF-R4

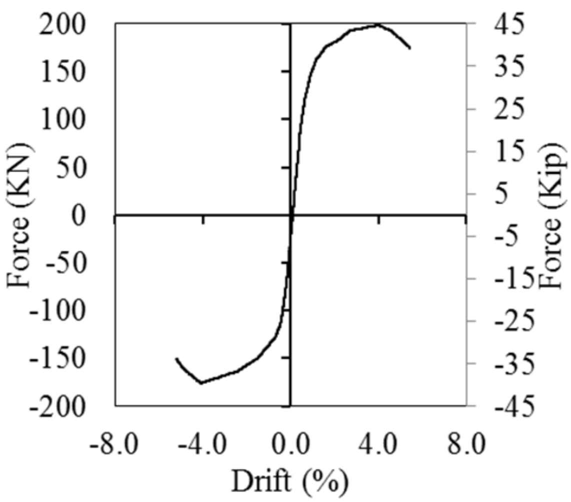

CF-R5

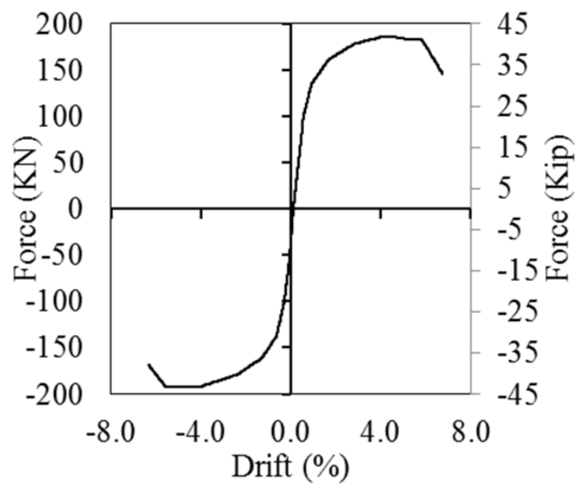

CF-R6

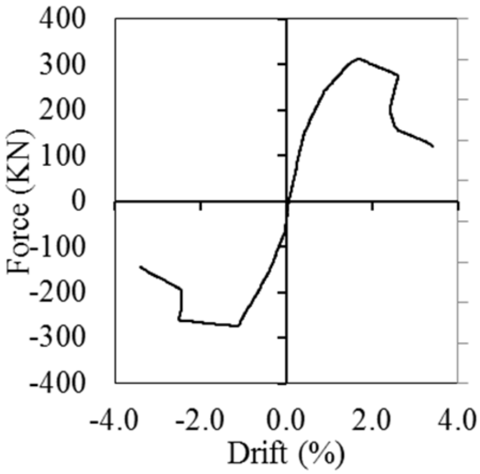

RF-R1

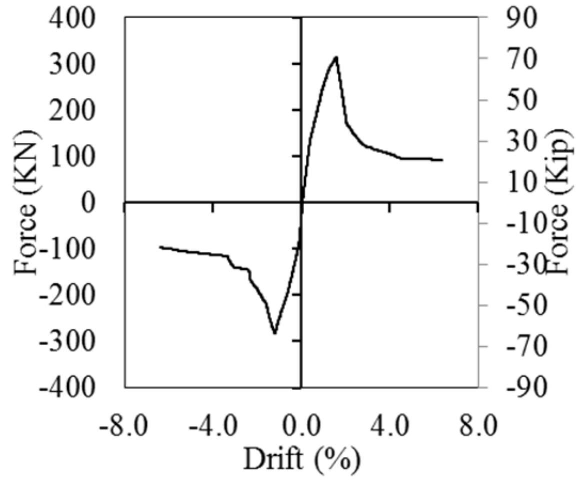

RF-R2

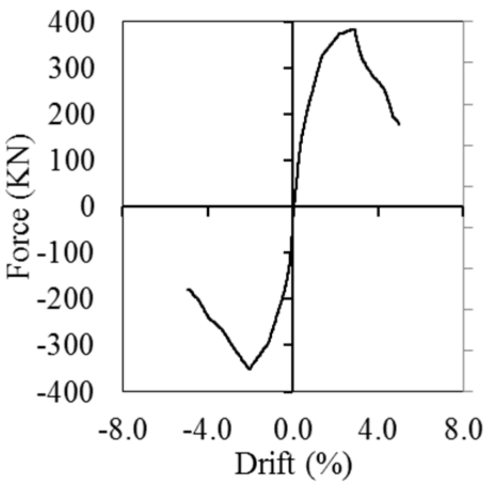

RF-R3

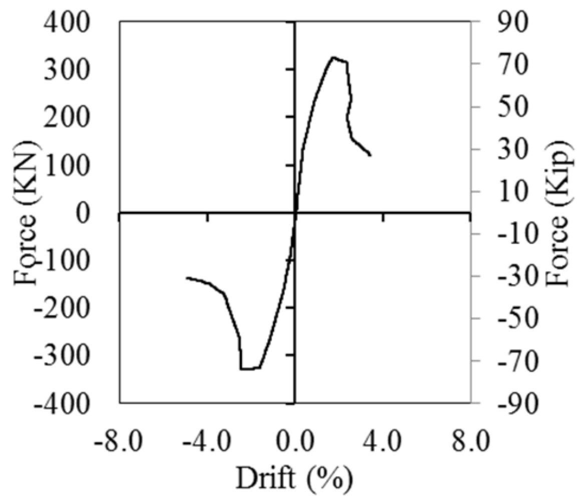

RF-R4

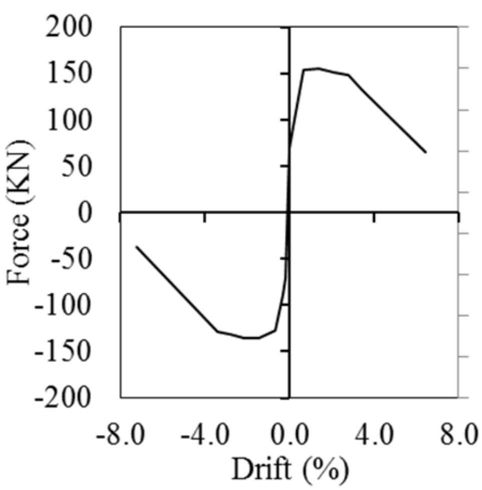

ASG-2NSS

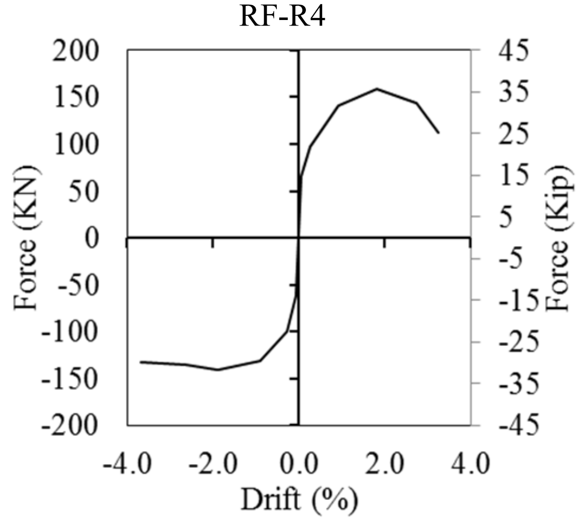

ASG-3NSS

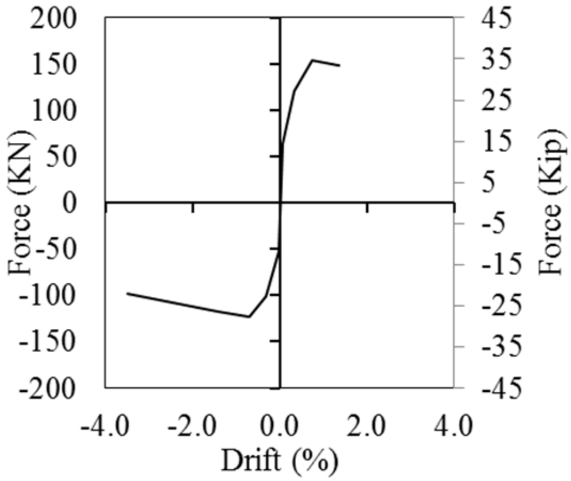

ASG-4NSS

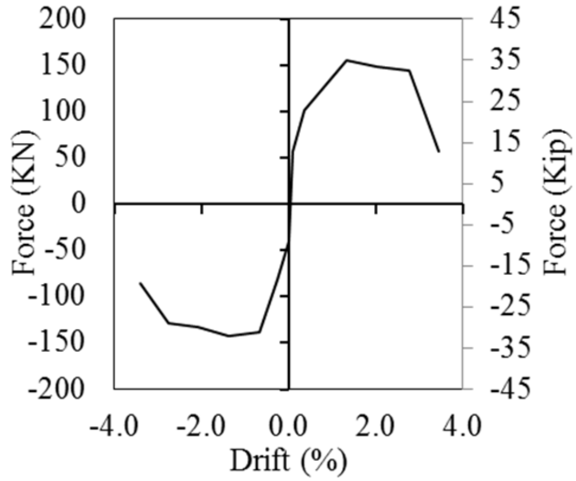

ASG-5NSS

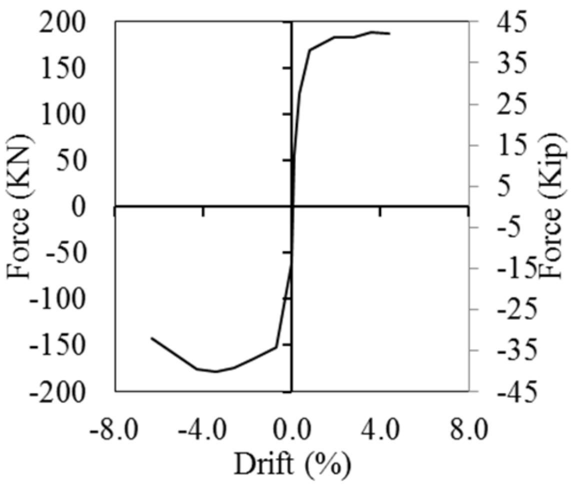

ASG-6NSS

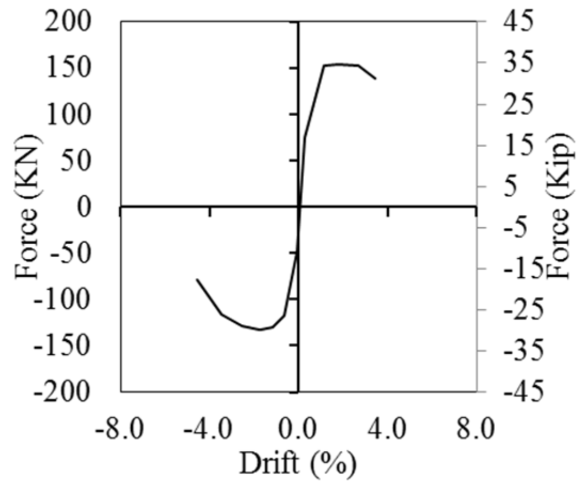

ASGR-7NSS

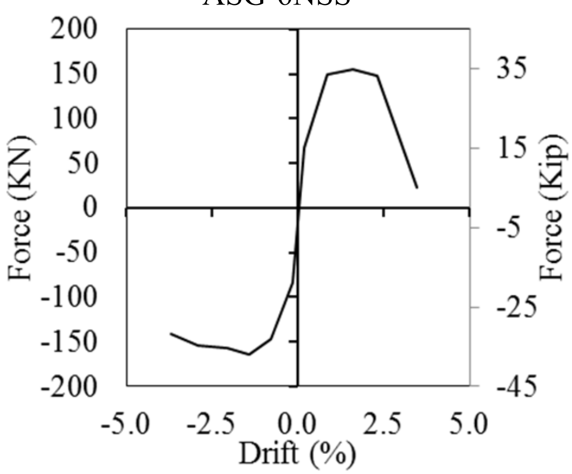

ASGR8NSS

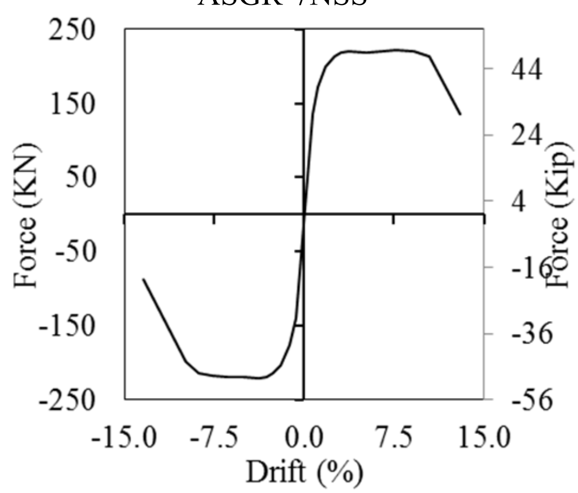

F2

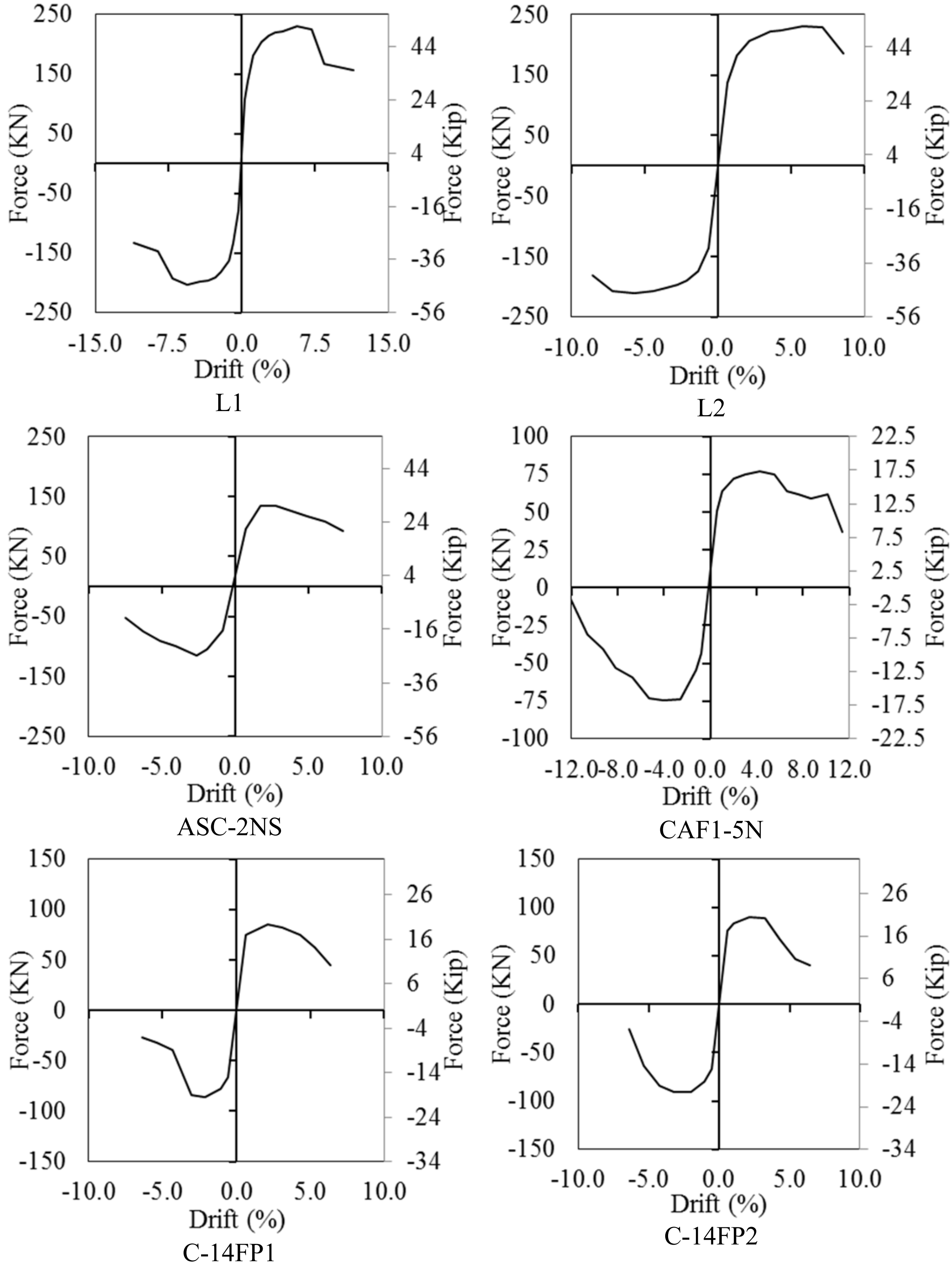
Force (KN)
Force (Kip)
Drift (%)
L1
L2
ASC-2NS
CAF1-5N
C-14FP1
C-14FP2
250
150
50
-50
-150
-250
44
24
4
-16
-36
-56
-15.0
-7.5
0.0
7.5
15.0
-10.0
-5.0
5.0
10.0
100
75
25
0
-25
-75
-100
22.5
17.5
12.5
7.5
2.5
-2.5
-7.5
-12.5
-17.5
-22.5
-12.0
-8.0
-4.0
4.0
8.0
12.0
-150
26
16
6
-4
-14
-24
-34

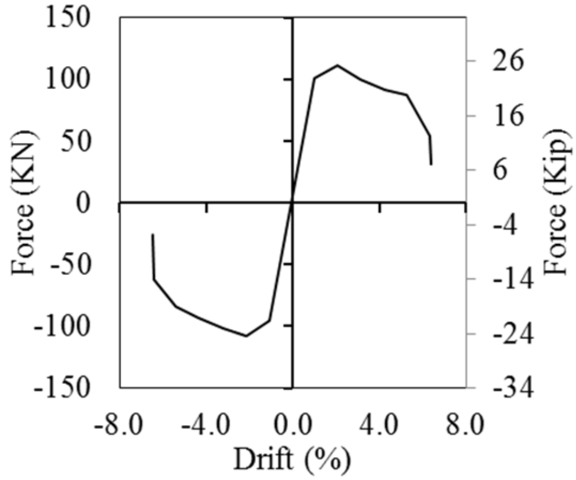

C-16FP1

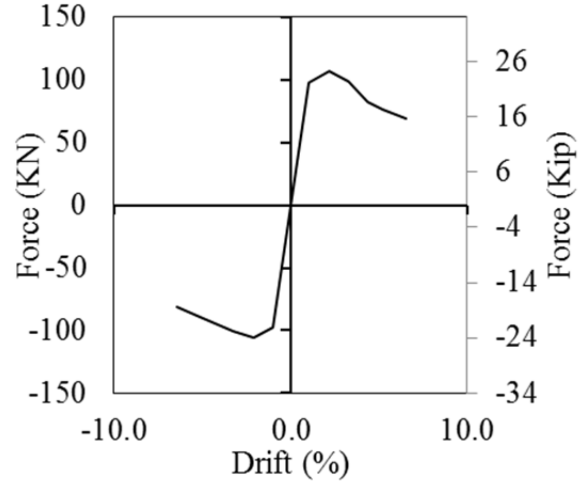

C-16FP2

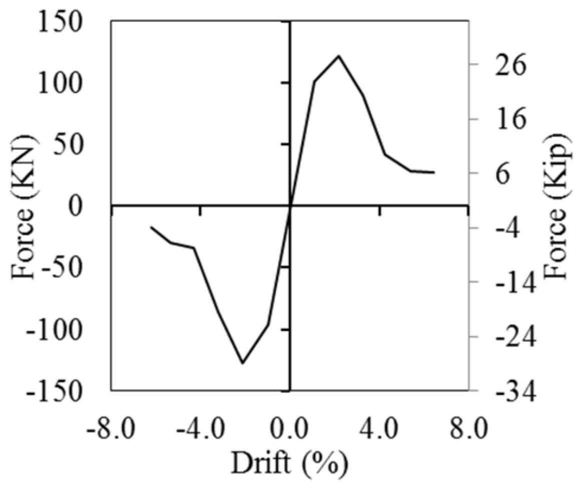

C-20-FP1

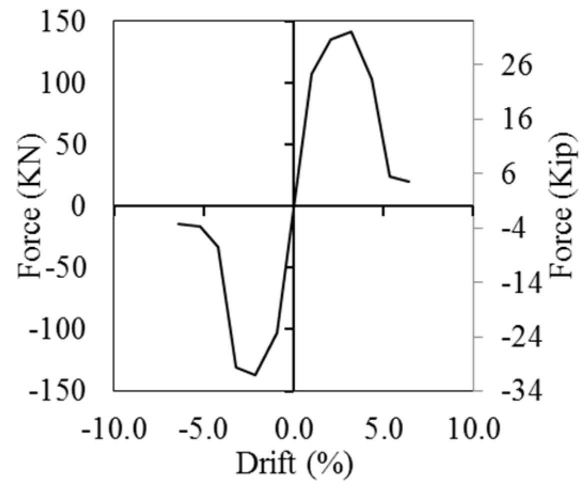

C-20-FP2

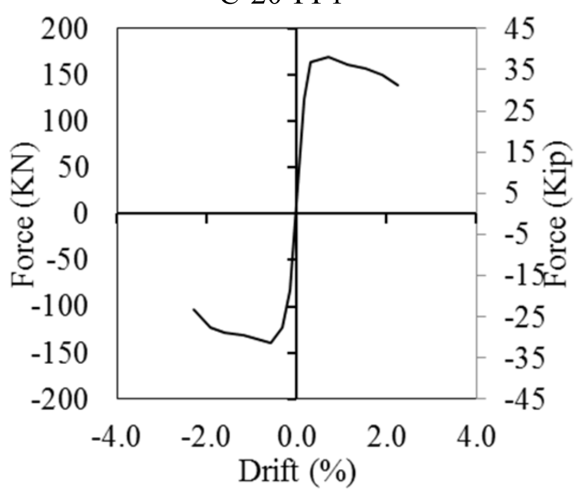

ASC-2NS

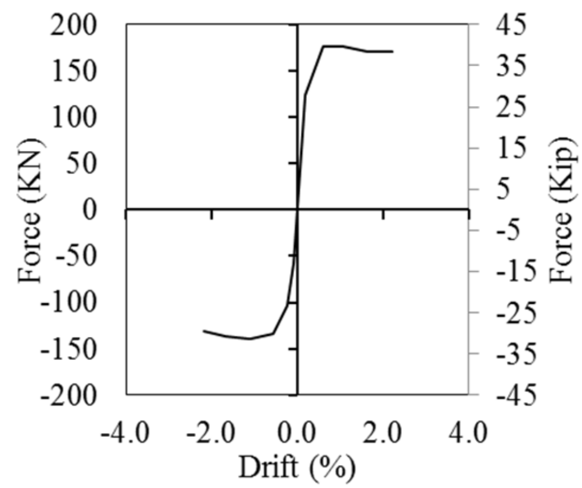

ASC-3NS

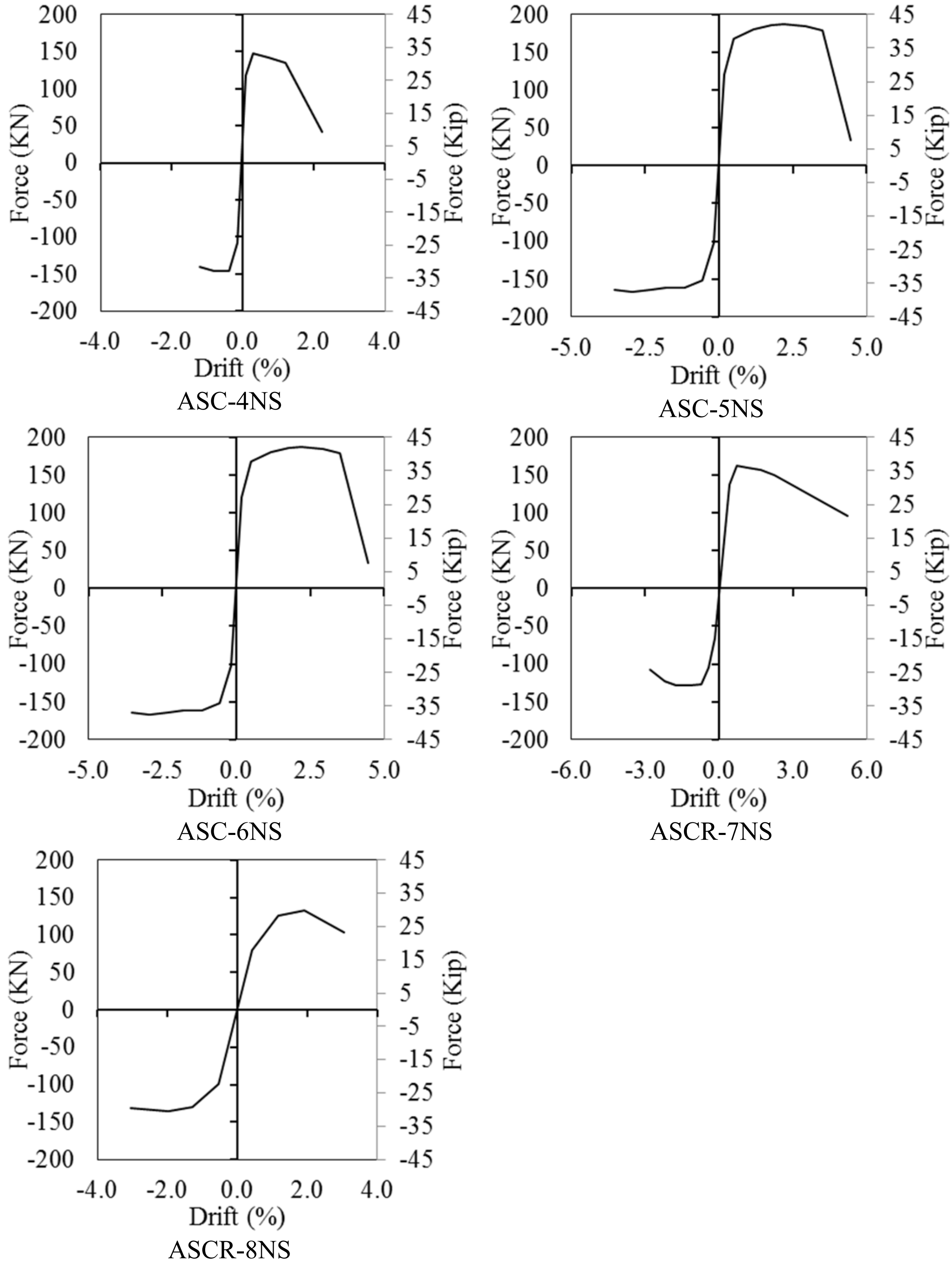

Steel Jacketed Reinforced Concrete Columns Backbones

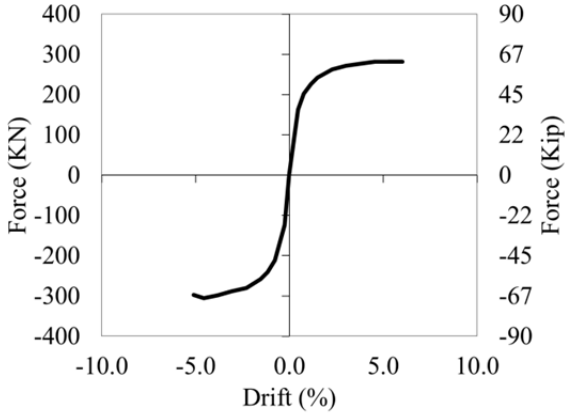

Chai 4

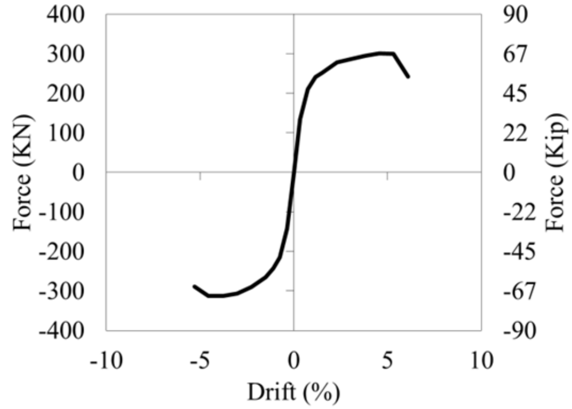

Chai 6

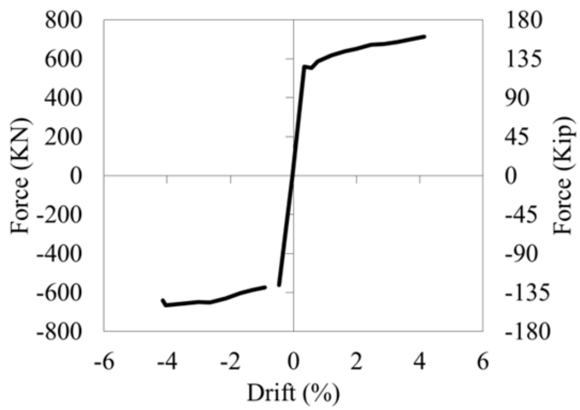

C2R

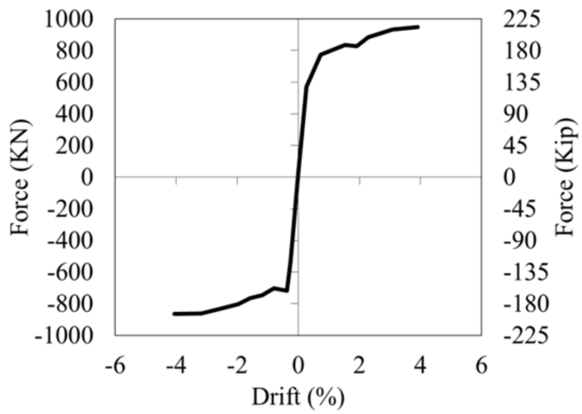

C4R

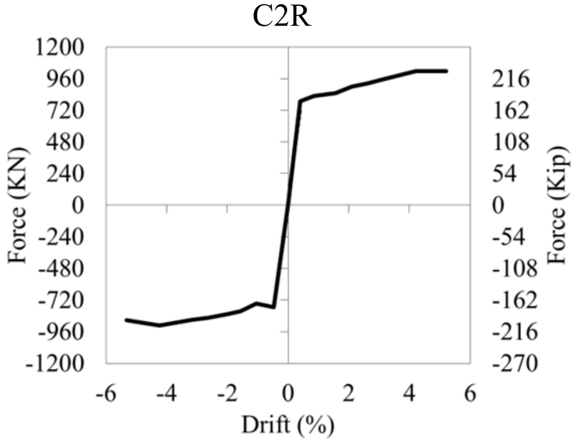

C6R

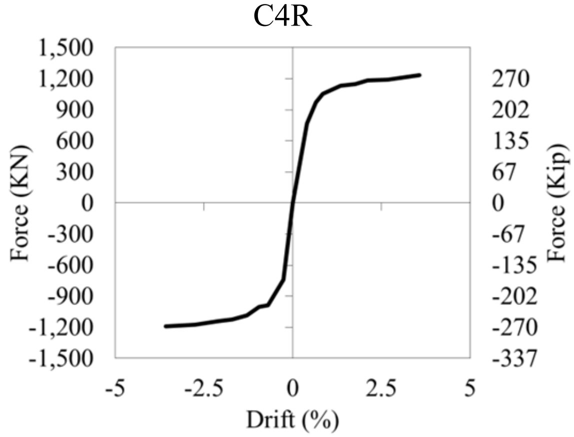

C8R

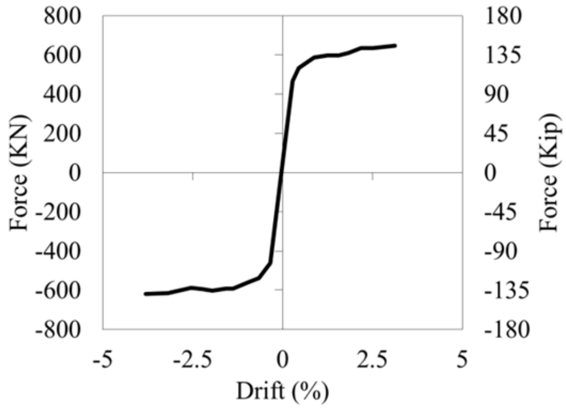

R2R

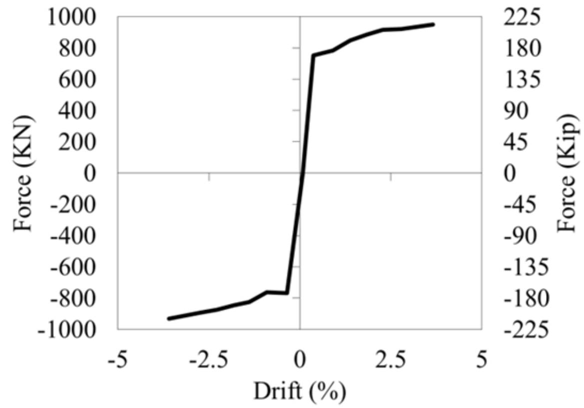

R4R

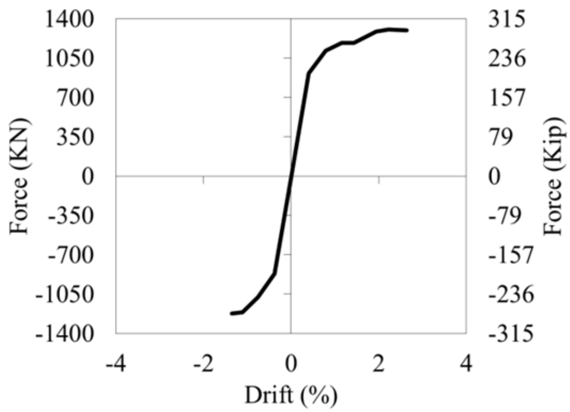

R6R

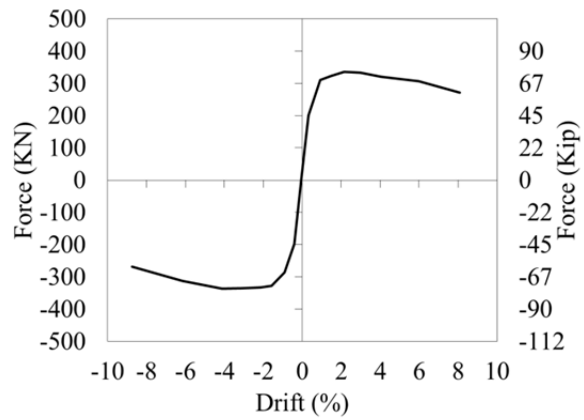

RC-5R

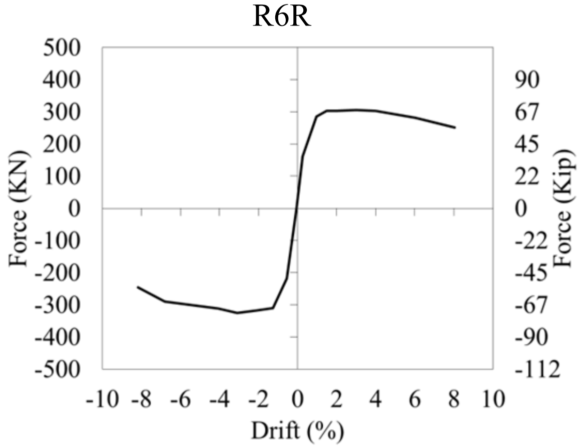

RC-4R

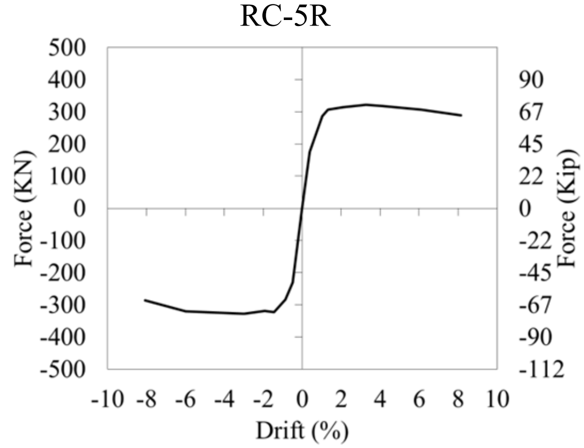

RC-3R

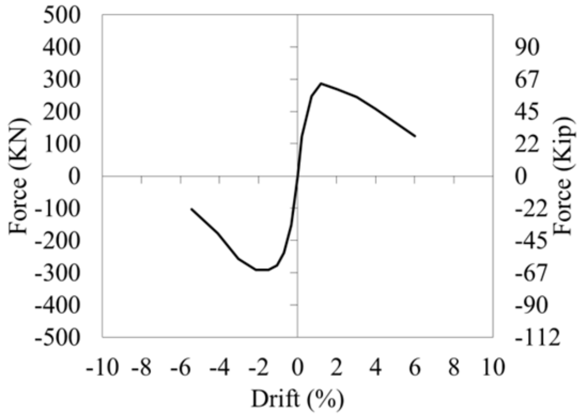

RC-2R

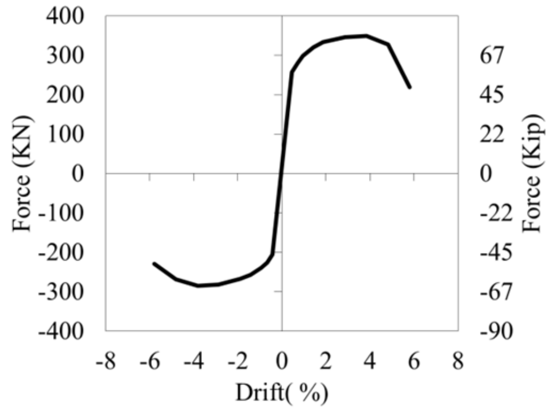

SC1

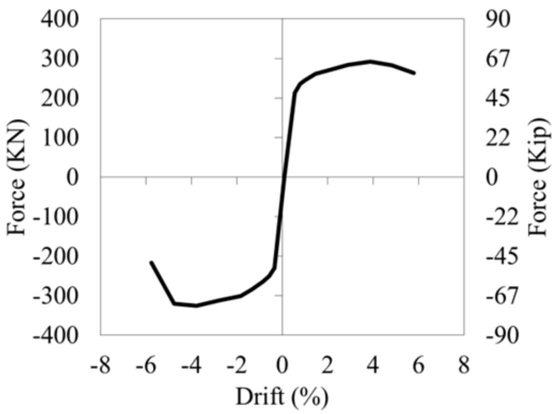

SC2

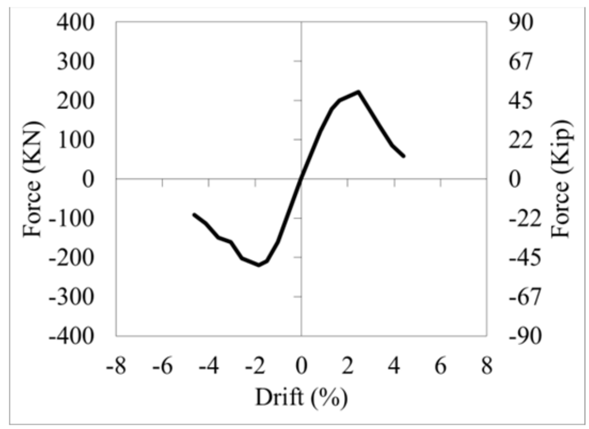

FC6

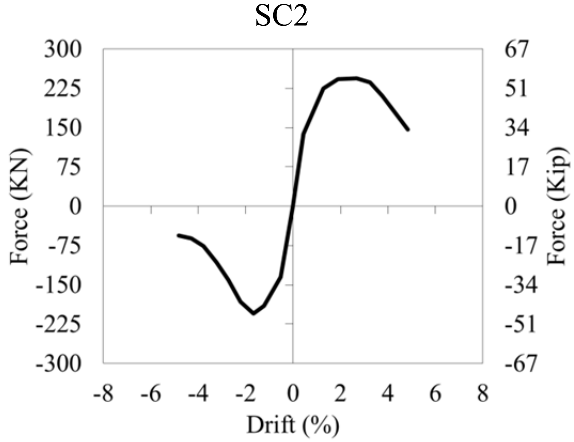

FC9

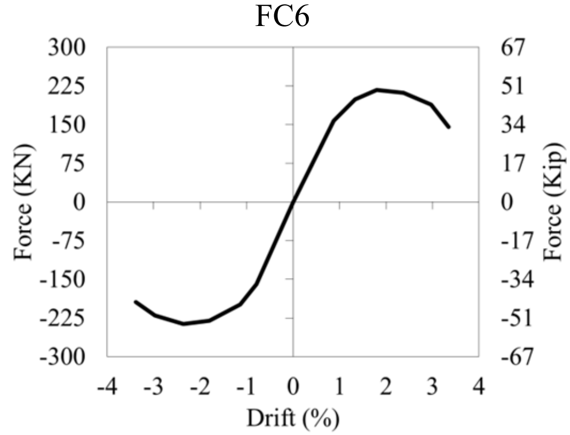

FC10

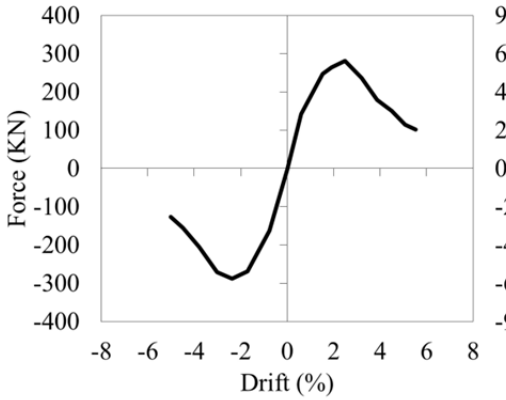

FC11

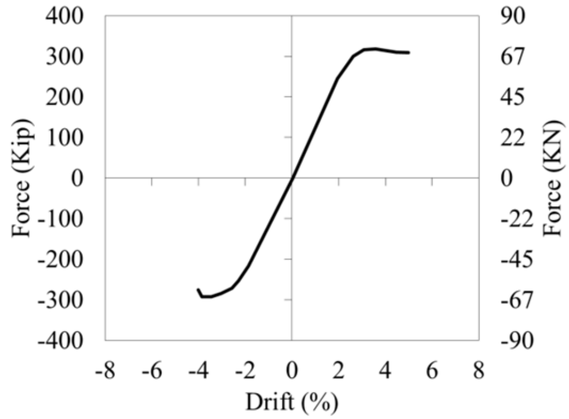

FC13

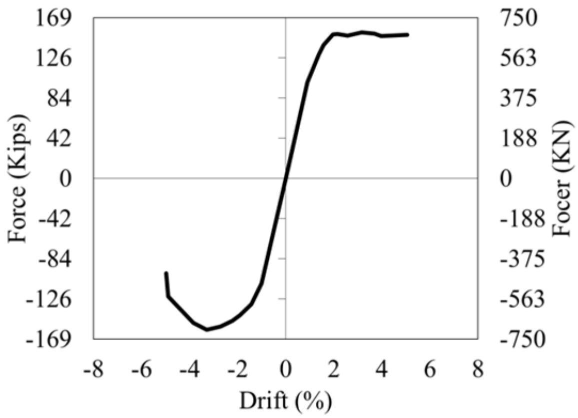

SC6

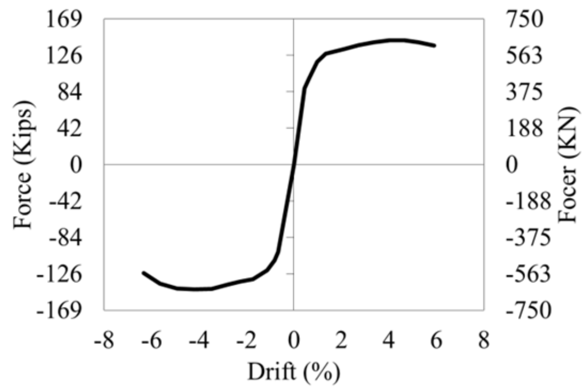

SC7

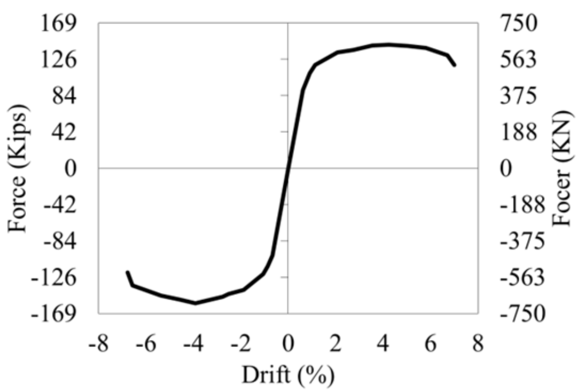

SC8

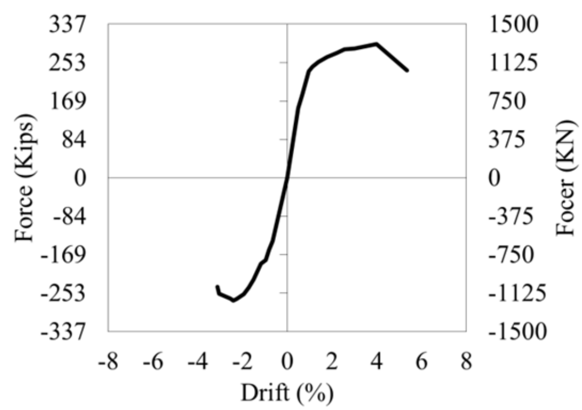

SC10

APPENDIX B: Column Database

Table 1 – Properties of jacketed columns in database: circular sections

Specimen	Reference	D_c (in)	Height (in)	f'_c (psi)	$P/A_g f'_c$	ρ (%)	ρ_v (%)	Deficient property*	V_y (kip)	V_{peak}/V_y	Δ_y/H (%)	Δ_p/H (%)	Δ_{max}/H (%)	Par. *a*	V_o/V_n
FRP-jacketed circular columns															
CFRP-05	Breña and Schlick (2007)	9.5	37.5	3467	0.05	2.54	0.333	LS	9.4	1.4	1.9	6.0	9.2	6.1	0.44
KFRP-05		9.5	37.5	3467	0.05	2.54	0.333	LS	9.6	1.4	1.4	6.3	9.5	6.8	0.44
CFRP-15		9.5	37.5	3467	0.15	2.54	0.333	LS	9.1	1.8	1.3	6.0	9.2	7.9	0.46
KFRP-15		9.5	37.5	3467	0.15	2.54	0.333	LS	9.5	1.4	1.1	6.2	10.0	8.8	0.46
CF-R1	Haroun and Elsanadedy (2005)	24.0	135.0	5223	0.06	1.95	0.103	LS	25.4	1.4	0.4	5.3	6.4	6.0	0.76
CF-R2		24.0	135.0	5353	0.06	1.95	0.103	LS	28.3	1.4	0.4	4.4	5.9	5.5	0.76
CF-R3		24.0	135.0	4758	0.07	1.95	0.103	LS	31.2	1.4	0.5	3.8	5.6	5.1	0.76
CF-R4		24.0	135.0	5469	0.06	1.95	0.103	LS	30.7	1.4	0.4	3.9	5.9	5.5	0.76
CF-R5		24.0	135.0	5759	0.06	1.95	0.103	LS	31.1	1.3	0.5	3.9	5.9	5.4	0.76
CF-R6		24.0	135.0	4802	0.07	1.95	0.103	LS	30.3	1.4	0.4	4.8	7.0	6.6	0.76
CS-R1		24.0	96.0	5919	0.05	1.95	0.103	S	80.2	1.4	0.2	3.1	3.6	3.4	1.69
CS-R2		24.0	96.0	5687	0.05	1.95	0.103	S	83.2	1.4	0.2	3.0	3.7	3.5	1.69
CS-R3		24.0	96.0	4961	0.05	1.95	0.103	S	116.1	1.4	0.5	3.8	4.3	3.8	1.68
CS-R4		24.0	96.0	5455	0.06	1.95	0.103	S	112.1	1.4	0.5	2.1	3.1	2.5	1.68
CS-P1		24.0	96.0	5179	0.06	1.95	0.103	S	119.8	1.4	0.3	3.9	4.1	3.7	1.68
Lap Splice R	Priestley et al. (1994)	24.0	144.0	4998	0.18	2.53	0.103	LS	42.7	1.4	0.1	2.4	3.8	3.5	0.82
C2-RT4	Xiao and Ma (1997)	24.0	104.0	6501	0.05	1.94	0.103	LS	53.2	1.3	0.4	1.4	5.1	3.2	0.89
C3-RT5		24.0	104.0	6501	0.05	1.94	0.103	LS	52.7	1.4	0.4	2.5	5.0	3.7	0.89
C4-RP4		24.0	104.0	6501	0.05	1.94	0.103	LS	36.5	1.4	0.6	2.0	5.4	2.7	0.89
CAF1-2N	Ghosh and Sheikh (2007)	14.0	57.9	3611	0.05	1.71	0.275	LS	17.0	1.3	1.0	1.2	4.9	1.1	0.28
CAF1-5N		14.0	57.9	3640	0.27	1.71	0.275	LS	12.2	1.4	0.8	4.3	12.3	5.1	0.34
CBF1-6N		14.0	57.9	3843	0.05	1.71	1.032	LS	13.6	1.3	1.0	5.5	8.7	6.2	0.10
ST-4NT		14.0	57.9	6497	0.27	1.71	1.032	LS	25.7	1.3	1.8	3.9	9.0	7.2	0.14

Table 1 (cont.) – Properties of jacketed columns in database: circular sections

Specimen	Reference	D_c (in)	Height (in)	f'_c (psi)	$P/A_g f'_c$	ρ (%)	ρ_v (%)	Deficient property*	V_y (kip)	V_{peak}/V_y	Δ_y/H (%)	Δ_p/H (%)	Δ_{max}/H (%)	Par. *a*	V_o/V_n
Steel-jacketed circular columns															
2	Chai et al. (1991)	24.0	144.0	5601	0.16	2.53	0.174	C	38.8	1.4	0.8	2.5	2.5	1.7	0.78
4		24.0	144.0	5521	0.16	2.53	0.174	C	48.0	1.4	0.4	6.0	**	5.6	0.78
5		24.0	144.0	5095	0.17	2.53	0.174	C	36.8	1.3	0.4	1.1	6.0	2.9	0.78
6		24.0	144.0	5426	0.16	2.53	0.174	C	49.2	1.4	0.5	4.6	6.1	5.4	0.78
1-R		24.0	144.0	5541	0.16	2.53	0.174	C	38.0	1.4	0.9	2.7	5.1	3.9	0.78
SC1	Hwang (2005)	29.9	128.0	3699	0.11	1.32	0.072	C	54.9	1.4	0.4	3.8	5.8	4.5	0.35
SC2		29.9	128.0	3699	0.11	1.15	0.067	C	51.3	1.4	0.3	3.8	5.8	5.5	0.37
C2R	Priestley et al. (1994)	24.0	96.0	4931	0.06	2.53	0.082	S	115.4	1.4	0.3	4.4	†	4.1	1.26
C4R		24.0	96.0	5101	0.17	2.53	0.082	S	150.4	1.4	0.3	4.1	†	3.8	1.23
C6R		24.0	96.0	5801	0.05	2.53	0.082	S	160.9	1.4	0.4	5.5	†	5.1	1.73
C8R		24.0	72.0	4521	0.06	2.53	0.082	S	193.0	1.4	0.3	5.2	†	4.9	2.15

*S – shear deficient; C – inadequate confinement; LS – short lap splice

**Test was stopped at peak load.

†Test stopped at the maximum displacement capacity of the actuator.

Table 2 – Properties of jacketed columns in database: rectangular columns

Specimen	Reference	b_c (in)	h_c (in)	H (in)	f'_c (psi)	$P/A_gf'_c$	ρ (%)	ρ_v (%)	Deficient property*	V_y (kip)	V_{peak}/V_y	Δ_y/H (%)	Δ_p/H (%)	Δ_{max}/H (%)	Par. *a*	V_o/V_n
FRP-jacketed rectangular columns																
S2	Ozcan et al. (2010)	15.8	7.9	70.8	1450	0.15	2.84	0.448	C	8.6	1.2	0.2	3.0	7.2	4.0	0.45
S3		15.8	7.9	70.8	1523	0.15	2.84	0.448	C	9.4	1.3	0.3	2.0	4.8	2.7	0.46
S4		15.8	7.9	70.8	1305	0.15	2.84	0.448	C	7.7	1.4	0.2	2.4	4.6	2.9	0.44
S5		15.8	7.9	70.8	2249	0.15	2.84	0.448	C	14.1	1.2	0.3	1.0	6.0	2.5	0.51
Confinement R	Seible and Priestley (1997)	28.7	19.3	144.0	4998	0.14	4.65	0.128	C	107.2	1.4	0.4	2.7	3.3	2.8	1.13
Shear R		24.0	16.0	96.0	4998	0.06	2.52	0.154	S	97.9	1.2	0.1	1.5	2.3	2.1	2.10
C3	Wu et al. (2008)	7.9	7.9	52.0	6775	0.24	2.00	0.000	C	10.8	1.3	1.0	2.1	7.2	6.2	1.73
C4		7.9	7.9	52.0	6804	0.23	2.00	0.000	C	11.8	1.3	1.1	2.4	8.0	6.9	1.73
C5		7.9	7.9	52.0	5281	0.30	2.00	0.000	C	11.1	1.3	1.0	4.0	7.2	6.2	1.72
C6		7.9	7.9	52.0	5368	0.30	2.00	0.000	C	11.0	1.3	1.0	2.0	7.3	6.3	1.72
ASG-2NSS	Memon and Sheikh (2005)	12.0	12.0	58.0	6165	0.15	2.44	0.316	C	24.6	1.4	0.7	4.6	23.7	2.6	0.59
ASG-3NSS		12.0	12.0	58.0	6195	0.15	2.44	0.316	C	24.9	1.4	0.2	6.0	12.0	3.5	0.59
ASG-4NSS		12.0	12.0	58.0	6282	0.15	2.44	0.316	C	24.2	1.4	0.3	2.4	11.4	2.0	0.59
ASG-5NSS		12.0	12.0	58.0	6340	0.15	2.44	0.316	C	24.4	1.4	0.6	4.3	11.2	2.0	0.59
ASG-6NSS		12.0	12.0	58.0	6412	0.15	2.44	0.316	C	29.8	1.4	0.9	11.8	20.7	5.4	0.60
ASGR-7NSS		12.0	12.0	58.0	6412	0.15	2.44	0.316	C	24.2	1.4	0.5	5.8	14.9	2.6	0.60
ASGR-8NSS		12.0	12.0	58.0	6412	0.15	2.44	0.316	C	25.8	1.4	1.0	4.7	12.2	3.4	0.60
ASC-2NS	Iacobucci et al. (2003)	12.0	12.0	58.0	5295	0.15	2.44	0.321	C	30.4	1.3	0.3	0.7	2.3	1.3	0.53
ASC-3NS		12.0	12.0	58.0	5353	0.15	2.44	0.321	C	31.8	1.3	0.2	0.6	2.2	2.0	0.53
ASC-4NS		12.0	12.0	58.0	5353	0.15	2.44	0.321	C	26.7	1.3	0.1	0.3	2.2	0.7	0.53
ASC-5NS		12.0	12.0	58.0	5368	0.15	2.44	0.321	C	33.7	1.3	0.4	2.2	4.5	2.3	0.53
ASC-6NS		12.0	12.0	58.0	5368	0.15	2.44	0.321	C	31.0	1.3	0.2	0.8	3.8	1.7	0.53
ASCR-7NS		12.0	12.0	58.0	5368	0.15	2.44	0.321	C	29.3	1.3	0.4	0.7	5.2	2.5	0.53
ASCR-8NS		12.0	12.0	58.0	6136	0.15	2.44	0.321	C	24.5	1.3	0.6	2.0	3.0	2.3	0.55
F2	Harries et al. (2006)	18.0	18.0	70.1	3597	0.22	1.48	0.180	C	35.0	1.4	1.1	7.7	13.4	6.2	0.40
L1		18.0	18.0	70.1	4162	0.22	1.48	0.180	LS	36.2	1.4	1.0	5.6	11.4	6.0	0.65
L2		18.0	18.0	70.1	4162	0.22	1.48	0.180	LS	36.4	1.4	1.2	5.8	8.6	5.4	0.65

Table 2 (cont.) – Properties of jacketed columns in database: rectangular columns

Specimen	Reference	b_c (in)	h_c (in)	H (in)	f'$_c$ (psi)	$P/A_g f'_c$	ρ (%)	$ρ_v$ (%)	Deficient property*	V_y (kip)	V_{peak}/V_y	$Δ_y/H$ (%)	$Δ_p/H$ (%)	$Δ_{max}/H$ (%)	Par. *a*	V_o/V_n
RF-R1	Haroun and Elsanadedy (2005)	24.0	24.0	135.0	5135	0.06	2.14	0.103	LS	55.9	1.3	0.7	2.4	2.8	2.1	1.38
RF-R2		24.0	24.0	135.0	6078	0.05	2.14	0.103	LS	56.2	1.3	0.7	1.1	4.5	3.8	1.38
RF-R3		24.0	24.0	135.0	6122	0.05	2.14	0.103	LS	60.3	1.4	0.7	2.0	3.6	2.8	1.37
RF-R4		24.0	24.0	135.0	6122	0.05	2.14	0.103	LS	59.2	1.3	0.8	1.7	3.5	2.7	1.37
RS-R1		24.0	18.0	96.0	5527	0.06	2.04	0.137	S	107.0	1.3	0.2	1.7	4.7	3.5	1.85
RS-R2		24.0	18.0	96.0	5701	0.06	2.04	0.137	S	104.6	1.3	0.3	1.1	4.7	3.5	1.86
RS-R3		24.0	18.0	96.0	6383	0.06	2.04	0.137	S	105.1	1.3	0.2	1.5	4.4	4.1	1.88
RS-R4		24.0	18.0	96.0	6383	0.06	2.04	0.137	S	95.8	1.4	0.1	2.1	4.6	4.5	1.88
RS-R5		24.0	18.0	96.0	6383	0.06	2.04	0.137	S	97.2	1.4	0.2	2.5	4.2	4.0	1.88
RS-R6		24.0	18.0	96.0	6180	0.06	2.04	0.137	S	107.0	1.3	0.2	1.8	4.9	4.7	1.87
C1FP1	Harajli and Rteil (2004)	11.8	5.9	39.4	3061	0.23	1.72	0.354	LS	10.9	1.4	0.9	3.0	6.0	3.4	0.57
C1FP2		11.8	5.9	39.4	3148	0.22	1.72	0.354	LS	5.5	3.9	0.6	3.0	5.1	3.3	0.57
C1F1		11.8	5.9	39.4	3177	0.22	1.72	0.354	LS	12.5	1.3	0.9	2.0	5.0	2.5	0.58
C1F2		11.8	5.9	39.4	3163	0.22	1.72	0.354	LS	11.2	1.4	1.0	3.0	5.1	3.4	0.57
C2FP1		11.8	5.9	39.4	3061	0.27	3.56	0.354	LS	15.2	1.4	0.8	3.0	5.1	3.0	0.82
C2FP2		11.8	5.9	39.4	3148	0.26	3.56	0.354	LS	15.1	1.4	0.7	3.0	5.1	3.2	0.83
C2F1		11.8	5.9	39.4	3177	0.26	3.56	0.354	LS	15.6	1.4	0.8	3.1	5.0	3.4	0.83
C2F2		11.8	5.9	39.4	3163	0.26	3.56	0.354	LS	15.3	1.4	0.8	3.0	5.1	3.4	0.83
SAF1-10N	Ghosh and Sheikh (2007)	12.0	12.0	57.9	3887	0.33	2.44	0.321	LS	19.9	1.3	0.8	2.5	7.8	3.2	0.46
SBF1-11N		12.0	12.0	57.9	3916	0.05	2.44	1.205	LS	14.3	1.3	0.8	2.3	3.8	2.1	0.14
SBRF1-12N		12.0	12.0	57.9	3945	0.05	2.44	1.205	LS	10.2	1.4	1.9	3.9	8.1	3.5	0.14
ASC-2NS		12.0	12.0	57.9	5294	0.33	2.44	1.205	LS	24.3	1.3	0.8	1.7	7.5	2.8	0.18
C14FP1	Harajli and Dagher (2008)	15.7	7.9	59.1	5656	0.00	1.29	0.735	LS	15.4	1.3	0.6	2.1	6.4	2.8	0.15
C14FP2		15.7	7.9	59.1	5656	0.00	1.29	0.735	LS	16.3	1.3	0.5	3.2	6.4	3.8	0.15
C16FP1		15.7	7.9	59.1	7107	0.00	2.00	0.735	LS	20.0	1.3	0.9	2.1	6.5	2.3	0.23
C16FP2		15.7	7.9	59.1	7107	0.00	2.00	0.735	LS	19.3	1.3	0.9	2.2	6.5	3.8	0.23
C20FP1		15.7	7.9	59.1	4641	0.00	2.13	0.735	LS	22.8	1.3	1.0	2.1	6.5	2.2	0.26
C20FP2		15.7	7.9	59.1	4641	0.00	2.13	0.735	LS	25.5	1.3	1.0	3.2	6.4	2.9	0.26

Table 2 (cont.) – Properties of jacketed columns in database: rectangular columns

Specimen	Reference	b_c (in)	h_c (in)	H (in)	f'_c (psi)	$P/A_g f'_c$	ρ (%)	ρ_v (%)	Deficient property*	V_y (kip)	V_{peak}/V_y	Δ_y/H (%)	Δ_p/H (%)	Δ_{max}/H (%)	Par. *a*	V_o/V_n
SC2	Galal et al. (2005)	12.0	12.0	36.0	5658	0.14	6.11	0.904	S	76.6	1.3	0.1	1.8	5.7	5.6	1.47
SC1R		12.0	12.0	36.0	4932	0.16	6.11	0.904	S	72.8	1.2	0.3	1.8	5.8	3.8	1.45
SC2R		12.0	12.0	36.0	4932	0.16	6.11	0.904	S	76.4	1.3	0.3	1.8	4.2	2.4	1.45
SC1U		12.0	12.0	36.0	6238	0.12	6.11	0.904	S	45.4	2.2	0.1	0.9	5.6	3.2	1.49
SC3		12.0	12.0	36.0	5658	0.14	6.11	0.904	S	78.4	1.3	0.2	1.8	5.7	4.0	1.47
SC3R		12.0	12.0	36.0	4932	0.16	6.11	0.904	S	54.6	1.3	0.3	0.6	3.6	1.3	1.45
Steel-jacketed rectangular columns																
C-66-R	Alcocer and Durán (2002)	19.7	19.7	78.7	4047	0.15	2.44	0.142	C	42.0	1.4	1.0	2.5	**	1.5	0.40
C-66-S		19.7	19.7	78.7	4047	0.15	2.44	0.142	C	64.7	1.4	1.0	2.7	**	1.7	0.40
RC-2R	Xiao and Wu (2003)	10.0	10.0	40.0	8269	0.30	2.48	0.220	C	45.8	1.4	0.4	2.1	6.0	3.1	0.30
RC-3R		10.0	10.0	40.0	8269	0.30	2.48	0.220	C	51.4	1.4	0.5	3.0	8.0	7.5	0.30
RC-4R		10.0	10.0	40.0	8269	0.30	2.48	0.220	C	50.9	1.4	0.4	3.1	8.0	6.8	0.30
RC-5R		10.0	10.0	40.0	8704	0.30	2.48	0.220	C	52.7	1.4	0.4	3.1	8.5	8.1	0.31
FC9	Aboutaha et al. (1996)	18.0	36.0	144.0	2906	0.00	1.95	0.095	LS	38.4	1.4	0.5	2.7	4.9	3.2	1.03
FC11		18.0	36.0	144.0	2851	0.00	1.95	0.095	LS	45.4	1.4	0.8	2.4	5.5	2.5	1.02
FC12		18.0	36.0	144.0	3266	0.00	1.95	0.095	LS	43.1	1.4	0.6	2.7	5.5	3.7	1.03
FC17		18.0	18.0	144.0	2636	0.00	1.95	0.076	LS	45.6	1.4	0.2	2.4	5.4	5.2	0.59
FC6	Aboutaha et al. (1999b)	18.0	36.0	144.0	2851	0.00	1.95	0.095	LS	34.9	1.4	1.0	2.5	4.6	2.2	1.02
FC7		18.0	36.0	144.0	2981	0.00	1.95	0.153	LS	52.0	1.4	1.5	3.9	**	2.4	0.69
FC10		18.0	36.0	144.0	2596	0.00	1.95	0.095	LS	37.2	1.4	0.8	2.4	3.4	2.6	1.02
FC13		18.0	36.0	144.0	3266	0.00	1.95	0.095	LS	50.0	1.4	0.4	3.6	5.0	4.6	1.03
SC6	Aboutaha et al. (1999a)	18.0	36.0	48.0	2256	0.00	1.95	0.095	S	111.1	1.4	1.0	3.3	5.1	3.2	1.32
SC7		18.0	36.0	48.0	2941	0.00	1.95	0.095	S	101.2	1.4	0.5	4.2	6.3	5.8	1.36
SC8		18.0	36.0	48.0	2786	0.00	1.95	0.095	S	109.7	1.4	0.7	3.9	7.0	5.8	1.35
SC10		36.0	18.0	48.0	2391	0.00	1.95	0.191	S	205.2	1.4	0.6	4.0	5.3	4.7	0.70

Table 2 (cont.) – Properties of jacketed columns in database: rectangular columns

R2R	Priestley et al. (1994)	16.0	24.0	96.0	5601	0.05	2.52	0.163	S	104.4	1.4	0.3	3.6	†	3.3	2.13
R4R		16.0	24.0	96.0	5201	0.06	2.52	0.082	S	154.7	1.4	0.3	3.8	†	3.5	2.88
R6R		16.0	24.0	72.0	4801	0.06	2.52	0.082	S	205.6	1.4	0.4	3.7	†	3.3	3.76

*S – shear deficient; C – inadequate confinement; LS – short lap splice

**Test stopped when capacity of actuator was reached.

†Test stopped at the maximum displacement capacity of the actuator.